Received: 2 October 2017 | Revised: 18 January 2018 | Accepted: 29 January 2018

DOI: 10.1002/humu.23408

RESEARCH ARTICLE

WILEY HGVS HUMAN GENOME VARIATION SOCIETY

Very short DNA segments can be detected and handled by the repair machinery during germline chromothriptic chromosome reassembly

Zuzana Slamova[1] | Lusine Nazaryan-Petersen[2] | Mana M. Mehrjouy[2] | Jana Drabova[1] | Miroslava Hancarova[1] | Tatana Marikova[1] | Drahuse Novotna[1] | Marketa Vlckova[1] | Zdenka Vlckova[3] | Mads Bak[2] | Zuzana Zemanova[4] | Niels Tommerup[2] | Zdenek Sedlacek[1]

[1]Department of Biology and Medical Genetics, Charles University 2nd Faculty of Medicine and University Hospital Motol, Prague, Czech Republic

[2]Wilhelm Johannsen Centre for Functional Genome Research, Department of Cellular and Molecular Medicine, University of Copenhagen, Copenhagen, Denmark

[3]GHC Genetics, Prague, Czech Republic

[4]Institute of Medical Biochemistry and Laboratory Diagnostics, General University Hospital and Charles University 1st Faculty of Medicine, Prague, Czech Republic

Correspondence
Zdenek Sedlacek, Department of Biology and Medical Genetics, Charles University 2nd Faculty of Medicine and University Hospital Motol, Plzenska 130/221, 15000 Prague 5, Czech Republic.
Email: zdenek.sedlacek@lfmotol.cuni.cz

Funding Information
Ministry of Health of the Czech Republic, Grant/Award Numbers: 17-29423A, 00064165, 00064203; Ministry of Education of the Czech Republic, Grant/Award Number: LM2015091; The Lundbeck Foundation, Grant/Award Number: 2013-14290; University of Copenhagen's Programme for Interdisciplinary Research, Grant/Award "Global Genes, Local Concerns"; The Danish Council for Independent Research - Medical Sciences, Grant/Award Number: 4183-00482B.

Communicated by David N. Cooper

Abstract

Analyses at nucleotide resolution reveal unexpected complexity of seemingly simple and balanced chromosomal rearrangements. Chromothripsis is a rare complex aberration involving local shattering of one or more chromosomes and reassembly of the resulting DNA segments. This can influence gene expression and cause abnormal phenotypes. We studied the structure and mechanism of a seemingly balanced de novo complex rearrangement of four chromosomes in a boy with developmental and growth delay. Microarray analysis revealed two paternal de novo deletions of 0.7 and 2.5 Mb at two of the breakpoints in 1q24.3 and 6q24.1-q24.2, respectively, which could explain most symptoms of the patient. Subsequent whole-genome mate-pair sequencing confirmed the chromothriptic nature of the rearrangement. The four participating chromosomes were broken into 29 segments longer than 1 kb. Sanger sequencing of all breakpoint junctions revealed additional complexity compatible with the involvement of different repair pathways. We observed translocation of a 33 bp long DNA fragment, which may have implications for the definition of the lower size limit of structural variants. Our observations and literature review indicate that even very small fragments from shattered chromosomes can be detected and handled by the repair machinery during germline chromothriptic chromosome reassembly.

KEYWORDS

alternative non-homologous end joining, chromothripsis, complex chromosome aberration, DNA repair, small insertions, whole-genome sequencing

1 | INTRODUCTION

Complex chromosome rearrangements (CCRs) are structural variations (SVs) involving more than two chromosome breaks and resulting in exchanges of chromosomal segments (Poot & Haaf, 2015). Balanced CCRs not accompanied by severe phenotypes can be transmitted in families where they can cause reproductive failure or birth of affected offspring due to unbalanced constitution of some gametes (Bertelsen et al., 2016; de Pagter et al., 2015; Pellestor et al., 2011; Pellestor, Gatinois, Puechberty, Genevieve, & Lefort, 2014). Carriers of apparently balanced CCRs can suffer from intellectual disability (ID), congenital defects or other disorders, due to gene truncations or fusions, positional effects, or submicroscopic deletions or other rearrangements at the breakpoints (Poot & Haaf, 2015; Weckselblatt & Rudd, 2015).

Analyses at nucleotide resolution usually reveal much higher complexity of CCRs (Redin et al., 2017). Some CCRs have the nature of germline chromothripsis, a phenomenon of multiple breakpoints and rearrangements clustering within small regions on one or

several chromosomes (Kloosterman et al., 2011; Kloosterman et al., 2012; Stephens et al., 2011). A likely main cause of chromothripsis is the missegregation of chromosomes into micronuclei or the formation of chromatin bridges by dicentric chromosomes, which induce chromosome fragmentation, and subsequent fusion of the segments via non-homologous end joining (NHEJ), although the exact mechanisms are not known. The double-strand breaks could be initiated by ionizing radiation, breakage-fusion-bridge cycles due to telomere attrition, aborted apoptosis, or endogenous endonucleases, and their clustered nature could result from shattering of highly condensed chromosomal regions during mitosis, or the spatial organization of interphase DNA (Ly & Cleveland, 2017; Ly et al., 2017; Nazaryan-Petersen & Tommerup, 2016). In addition to the classical NHEJ, the participation of alternative NHEJ mechanisms in structural genetic variation in mammalian cells has been described, including the error-prone microhomology-mediated end joining (MMEJ) (Seol, Shim, & Lee, 2017; Sfeir & Symington, 2015). Other mechanisms of CCRs such as chromoanasynthesis likely involve also replication-associated events showing microhomology at newly formed junctions such as fork stalling and template switching (FoSTeS) and microhomology-mediated break-induced replication (MMBIR) (Liu et al., 2011).

Germline chromothripsis can deregulate many genes in a broad neighborhood of the breakpoints (Middelkamp et al., 2017), and can be associated with a range of genetic diseases, mainly with ID and developmental defects (Collins et al., 2017; Nazaryan-Petersen & Tommerup, 2016; Redin et al., 2017).

We studied a boy with developmental and growth delay in whom karyotyping revealed a seemingly balanced de novo CCR involving chromosomes 1, 6, 14, and 18. Multicolor fluorescent in situ hybridization and chromosome banding (mFISH and mBAND) confirmed a CCR formed by a total of 11 segments. Microarray analysis identified de novo deletions of 0.7 and 2.5 Mb of paternal DNA at two of the breakpoints, in 1q24.3 and 6q24.1-q24.2, respectively. Both these regions have been associated with growth retardation and ID, and the deletions could explain most of the symptoms of the patient. Whole-genome mate-pair sequencing (MPS) showed that the CCR was even more complex, involving a total of 29 segments (four of which were deleted), and pointed to several additional genes affected by the breakpoints. Sanger sequencing of all newly formed segment junctions revealed additional complexity and showed that very short DNA segments of tens of base pairs can be formed during chromosome shattering, and that these short segments can behave the same way as megabase-long segments, that is, can be incorporated into the derivative chromosomes or lost. An implication of this is that at least some of the small deletions frequently seen at CCR breakpoints might reflect closely placed double-strand breaks.

2 | MATERIALS AND METHODS

2.1 | Patient

The boy was born as the first child of non-consanguineous parents aged 29 (mother) and 35 years (father) after an uncomplicated pregnancy. The delivery was spontaneous in the 35th week of gestation. Birth weight was 1,600 g and length was 43 cm (both < 5th centile). The perinatal adaptation was uncomplicated. Severe postnatal growth retardation and developmental delay were observed at the age of 1 year. The boy started walking at the age of 2 years and his psychomotor and speech development were mildly delayed. He was treated with growth hormone for several years. He enrolled a standard primary school with an assistant; however, his mental condition suddenly worsened. The regress was accompanied by disorientation and behavioral problems. He had a limited vocabulary and suffered from dysarthria. Physical examination of the patient at the age of 15 years showed severe growth retardation (height 152 cm, < 5th centile) and truncal obesity (weight 74 kg, 90th centile). He also showed a range of distinctive facial anomalies (narrow forehead, low hairline, hypotelorism, small palpebral fissures, synophrys, large nose with broad nasal bridge, long prominent philtrum, and atypically shaped large earlobes), and other abnormal physical features (short neck, massive shoulders and abdomen, severe thoracic kyphosis, lumbar hyperlordosis, short limbs, short fingers with pads, bilateral single transverse palmar flexion creases, genua valga, short toes, and a small penis [with a previous surgery of hypospadia]). Cardiological, sonographic, and MRI examinations found no abnormalities. The family history was insignificant, and the parents and a younger brother of the patient were healthy. The study was approved by the Ethics Committee of University Hospital Motol, Prague, and informed consent was obtained from the parents of the patient who are his legal guardians.

2.2 | Karyotyping, FISH, mFISH, and mBAND

G-banded metaphase chromosomes from cultured peripheral blood lymphocytes of the patient and his parents were prepared using standard protocols. Karyotyping was performed at a minimal resolution of 550 bands. To better understand the complexity of the CCR identified in the patient, mFISH was performed using the 24XCyte MetaSystems Color Kit (MetaSystems, Altlussheim, Germany) containing painting probes for all human chromosomes. mBAND analysis was performed using the XCyte 1 and XCyte 6 probes (MetaSystems). Additional FISH analyses used subtelomere 18p and chromosome18 centromere probes (Aquarius, Cytocell, Tarrytown, NY), locus-specific probes RP11-506O24 (1q23.3) and RP11-81H19 (1q24.3) (Empire Genomics, Buffalo, NY), and RP11-24L5 (18q12.3) (BlueGnome, Cambridge, UK) to confirm the structural rearrangements, define the breakpoints and verify the array findings. Between 15 and 30 mitoses were analyzed for all cytogenetic and molecular cytogenetic methods used.

2.3 | Microarray analysis and next generation whole-genome MPS

Genomic DNA of the patient and his parents was extracted from peripheral blood lymphocytes using the AutoGen Flex STAR extractor (AutoGen, Holliston, MA) and the FlexiGene DNA AGF Kit (Qiagen, Hilden, Germany), and analyzed using SNP array Human CytoSNP-12 BeadChips (~300K; Illumina, San Diego, CA). Nextera

MPS gel-free protocol was performed on genomic DNA of the patient as described earlier (Bertelsen et al., 2016). The final library was subjected to 2× 100 base paired-end sequencing on an Illumina HiSeq2500 sequencing platform, and mapped to the human reference genome (the whole study used build GRCh37/hg19) using BWA (Li & Durbin, 2009). Duplicate reads were removed using Picard Tools (https://broadinstitute.github.io/picard/) and reads with a mapping quality <10 were removed using Samtools (Li et al., 2009). The number of read pairs passing the alignment score was >26 million, corresponding to 17× genomic coverage. SVs were identified using SVDetect (Zeitouni et al., 2010) and Delly (Rausch et al., 2012). Only SVs with at least five confirming read-pairs were considered. To identify sample-specific SVs, the predicted SVs were compared with an in-house database containing SVs from 48 mate-pair analyzed samples. Rearrangements that were not unique to the present case (i.e., if the breakpoint regions of a predicted SV overlapped both breakpoint regions of an SV in the database) were excluded. All segment junctions were confirmed using PCR and Sanger sequencing.

3 | RESULTS

Chromosome analysis of the patient showed a male karyotype with derivative chromosomes 1, 6, 14, and 18 (Fig. 1A). Parental karyotypes were normal indicating that the CCR was de novo. Additional analyses using mFISH and mBAND (Fig. 1B–D) confirmed the involvement of 11 segments from the four participating chromosomes (Fig. 2, non-framed segment numbers), and yielded the karyotype t(1;6;14;18)(1pter→1q23::18p11.3→18pter;6pter→6q15::1q25→1q24::18q11.2→18qter;14pter→14q13?::6q24.2→6qter;1qter→1q25: :18p11.2→18q11.2::6q15→6q24::14q13?→14qter). The SNP array analysis revealed two interstitial deletions likely adjacent to two of the breakpoints, both of de novo origin and affecting paternal chromosomes. A 0.7 Mb long deletion in 1q24.3 involved four protein-coding RefSeq genes, *DNM3*, *PIGC*, *C1ORF105* and *SUCO*. A 2.5 Mb long deletion in 6q24.1-q24.2 removed 15 protein-coding RefSeq genes (*NMBR*, *VTA1*, *ADGRG6*, *HIVEP2*, *AIG1*, *ADAT2*, *PEX3*, *FUCA2*, *PHACTR2*, *LTV1*, *ZC2HC1B*, *PLAGL1*, *SF3B5*, *STX11* and *UTRN*). The SNP array analysis thus defined two segments, which were deleted (Fig. 2, red elliptical-framed segment numbers). The patient carried no additional significant copy number variants.

The MPS analysis of the patient not only confirmed the above mentioned findings, but also identified additional smaller rearrangements. The four chromosomes involved were in fact fragmented into a total of 29 segments longer than 1 kb (Fig. 2, the 16 segments identified uniquely by MPS are rectangle-framed; Supp. Figs. S1 and S2 and Supp. Table S1). The segments were inserted into the derivative chromosomes in a random order and orientation. At least two of the newly identified segments were lost, causing two additional breakpoint-associated deletions (Fig. 2, rectangle-framed red segment numbers). One of them spanned about 30 kb of 14q13.3 (chr14:37113581-37144087) and removed most of the *PAX9* gene. Another deletion, suspected from the MPS data and confirmed using PCR and Sanger sequencing, removed about 2 kb of 6q14.1 (chr6:77318764-77320990). The MPS analysis also defined the exact extent of the two large deletions identified previously using SNP arrays (chr1:171938643-172600557 and chr6:142164956-144627966).

Besides the genes affected by the deletions, five additional protein-coding RefSeq genes (*FILIP1*, *PHIP*, *HMGN3*, *AK097143*, and *GAREM*) were interrupted by the other breakpoints (Supp. Table S1). One of the breakpoint junctions led to a possible formation of a fusion gene (a fusion of the first exon of *GAREM* with the 3′ part of *HMGN3* starting with the second exon), which, however, did not preserve the reading frame (and it is unclear if its function could be restored at the level of splicing by skipping of some exons). None of the breakpoints affected known regulatory regions of genes known to be associated with long-range position effects (LRPE). Moreover, the large number of deleted and truncated genes would make it difficult to assess whether any of the breakpoints might be associated with new LRPE regions.

All 21 new breakpoint-junctions (No. 1–21) were confirmed and refined using PCR and Sanger sequencing (Supp. Table S1). Of the total of 17 chromosome breaks where both originally adjacent segments were included in the derivative chromosomes, a completely balanced state could be identified at six segment boundaries, duplications of 2, 3, and 4 bp at three segment boundaries, deletions of 1, 3, 7, 10, 29, 31, and 33 bp at seven segment boundaries, and two deletions of 59 and 18 bp separated by 12 bp of DNA at one boundary (Supp. Table S1). Of the 21 new segment junctions, microhomology of 1–6 bases could be observed at thirteen junctions, no microhomology at seven junctions and one junction (No. 20) was highly complex with deletions of 31 and 59 + 18 bp at the ends of the participating segments. Surprisingly, the stretch of 33 bp seemingly deleted from another junction was not lost but was inserted into junction No. 20, together with an additional insertion of 20 bp of DNA that could not be mapped to the reference genome (Fig. 3 and Supp. Table S1). Chromothripsis has been associated with transgene integration (Chiang et al., 2012) and recently with a de novo retroelement insertion at one of the breakpoints (Nazaryan-Petersen et al., 2016), but no signature of retroposition could be identified at the breakpoints of this CCR.

4 | DISCUSSION

We describe the analysis of a de novo CCR showing hallmarks of germline chromothripsis and affecting four chromosomes in a patient with growth retardation, ID, delayed speech development, and facial and other somatic abnormalities. Although the CCR was originally considered balanced, the SNP array analysis identified two large deletions of 1q24.3 and 6q24.1-q24.2, which can explain most, if not all of the symptoms seen in the patient. This is in line with previous observations that phenotypic abnormalities in carriers of apparently balanced de novo CCRs can be caused by cryptic deletions at the breakpoints (De Gregori et al., 2007).

Deletions overlapping the 1q24.3 deletion of our patient have been described, and most were associated with ID, intrauterine and postnatal growth retardation, short limbs, brachydactyly, and distinctive facial

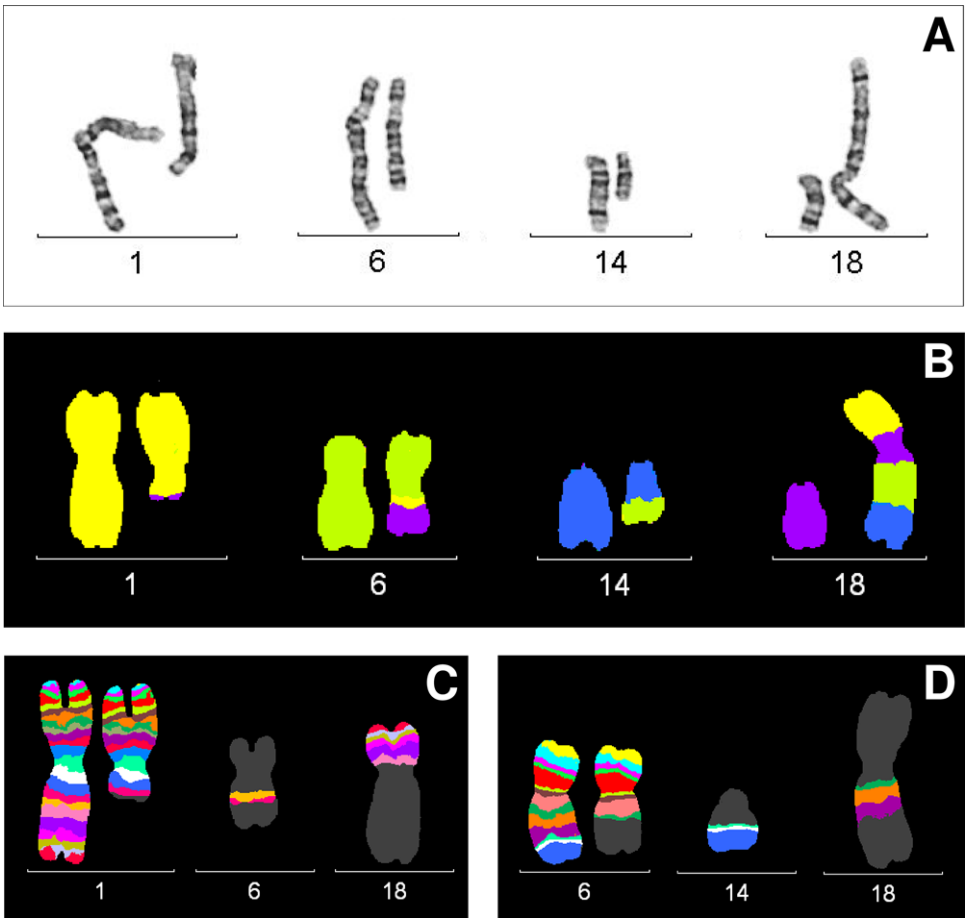

FIGURE 1 Partial karyotype (A) and mFISH (B) and mBAND profiles using mBAND probes for chromosome 1 (C) and chromosome 6 (D) of the derivative chromosomes of the patient. These analyses originally identified 11 chromosome segments participating in the CCR

features (Ashraf et al., 2015; Chatron et al., 2015), symptoms consistent with those observed in our patient. His deletion was 0.7 Mb long and it was among the smallest reported. It contained the 0.5 Mb long critical region of the 1q24-q25 deletion syndrome spanning the *DNM3* gene and the *miR-199/214/3120* cluster located in one of the *DNM3* introns (Ashraf et al., 2015; Chatron et al., 2015). *DNM3* encodes dynamin 3, a protein expressed in brain and spinal cord, which interacts with the Homer-Shank scaffold complex in postsynaptic hippocampal neurons. The Homer-Shank complex and dynamin 3 are involved in clathrin-coated vesicle endocytic machinery, recycling of receptors back to the synapse and increasing of synaptic strength (Lu et al., 2007; Romeu & Arola, 2014). The deletion of *DNM3* and *miR-199/214/3120* is likely the key factor contributing to the growth and mental impairment as well as to skeletal features observed in the patients (Ashraf et al., 2015; Chatron et al., 2015). The neighboring *PIGC* gene encodes the class C phosphatidylinositol glycan, an endoplasmic reticulum protein involved in the biosynthesis of glycosylphosphatidylinositol (GPI) anchors in transmembrane proteins. Its recessive defects cause embryonic lethality (Shamseldin et al., 2015). Mutations in other genes involved in GPI biosynthesis are associated with neurological features, epilepsy, and ID (Freeze, Eklund, Ng, & Patterson, 2015), as are mutations in another gene deleted in our patient, *SUCO*, encoding the SUN domain containing ossification factor (Sha et al., 2015). The contribution of *PIGC* and *SUCO* to the phenotype of our patient is unclear.

The other large deletion affected 2.5 Mb of 6q24.1-q24.2. Several rare 6q24-q25 deletions described in the literature were much larger and located more distally (Stagi et al., 2015), making a direct comparison difficult. Interestingly, the deletion in our patient affected the paternal copy of 6q24.1-q24.2, supporting the notion that the CCR in our patient is also likely to be of paternal origin as reported in previous cases of de novo constitutional chromothripsis (Weckselblatt & Rudd, 2015; Weckselblatt, Hermetz, & Rudd, 2015). The 6q24.1-q24.2 region is known to contain two maternally imprinted genes, *PLAGL1* (pleiomorphic adenoma gene-like 1) and *HYMAI* (hydatidiform mole associated and imprinted). Defects of this imprinted domain have been associated with transient neonatal diabetes mellitus and failure to thrive (Arima et al., 2001), and most deletion patients showed intrauterine and postnatal growth retardation, developmental delay and facial dysmorphism (Stagi et al., 2015). Mice with inactivated paternal allele of the *PLAGL1* homologue showed prenatal growth restriction and bone defects (Varrault et al., 2006). The deletion contained several other candidate genes possibly contributing to the phenotype of our patient. For example, *HIVEP2* encodes the HIV type I enhancer-binding protein 2, and de novo mutations in this gene have been identified in ID patients (Srivastava et al., 2016; Steinfeld et al., 2016).

The breakpoints identified using MPS affected additional genes. Among them, *PHIP*, encoding pleckstrin homology domain-interacting

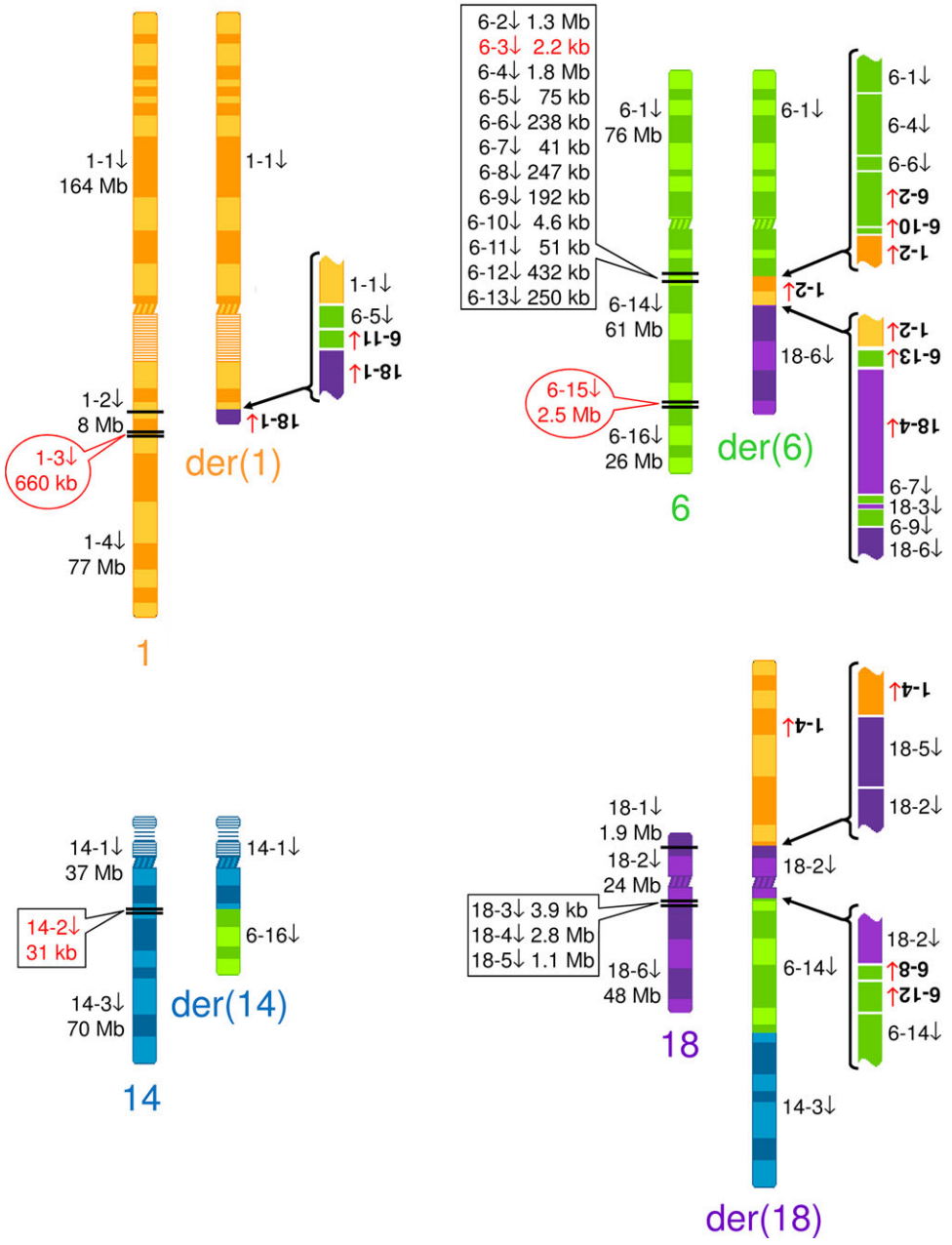

FIGURE 2 Schematics of the CCR. The ideograms of the normal chromosome homologues show the segments participating in the rearrangement and their size. Segments identified using karyotyping, mFISH and mBAND are not framed. Segments identified using microarrays are in elliptical frames, and segments identified using MPS are in rectangular frames. Deleted segments not present in the CCR are indicated in red. The rearrangements identified using karyotyping, mFISH and mBAND are shown on the ideograms of the derivative chromosomes. Segments inserted in the inverted orientation are indicated in bold with red upward arrows. Regions shown to be more complex using MPS are depicted in enlarged figures

protein, is the most interesting as it belongs to strong candidate ID genes (de Ligt et al., 2012). One of the deletions in our patient inactivated one copy of the *PAX9* gene, which has been associated with tooth agenesis. Our patient did not show symptoms of this condition, similarly to several other patients with *PAX9* deletions in the DECIPHER database (Firth et al., 2009). As this phenotype is unlikely to be underreported, incomplete penetrance or a more specific disease mechanism must be considered in this condition.

Our patient illustrates how the gradual employment of methods with increasing resolution leads to the revelation of increasing complexity of a CCR, which was originally considered to be much simpler (and balanced). This refinement has consequences for the genotype–phenotype correlation, as it broadens the list of candidate genes affected by the CCR that could be responsible for the symptoms observed, and also for possible mechanisms of the rearrangement.

The CCR of our patient shows hallmarks of chromothripsis with clustering of multiple breakpoints in several chromosome regions (with more breaks on each chromosome involved) and random rearrangement of the segments with just a few deletions and no duplications or triplications. Most of the junctions show features of NHEJ such as

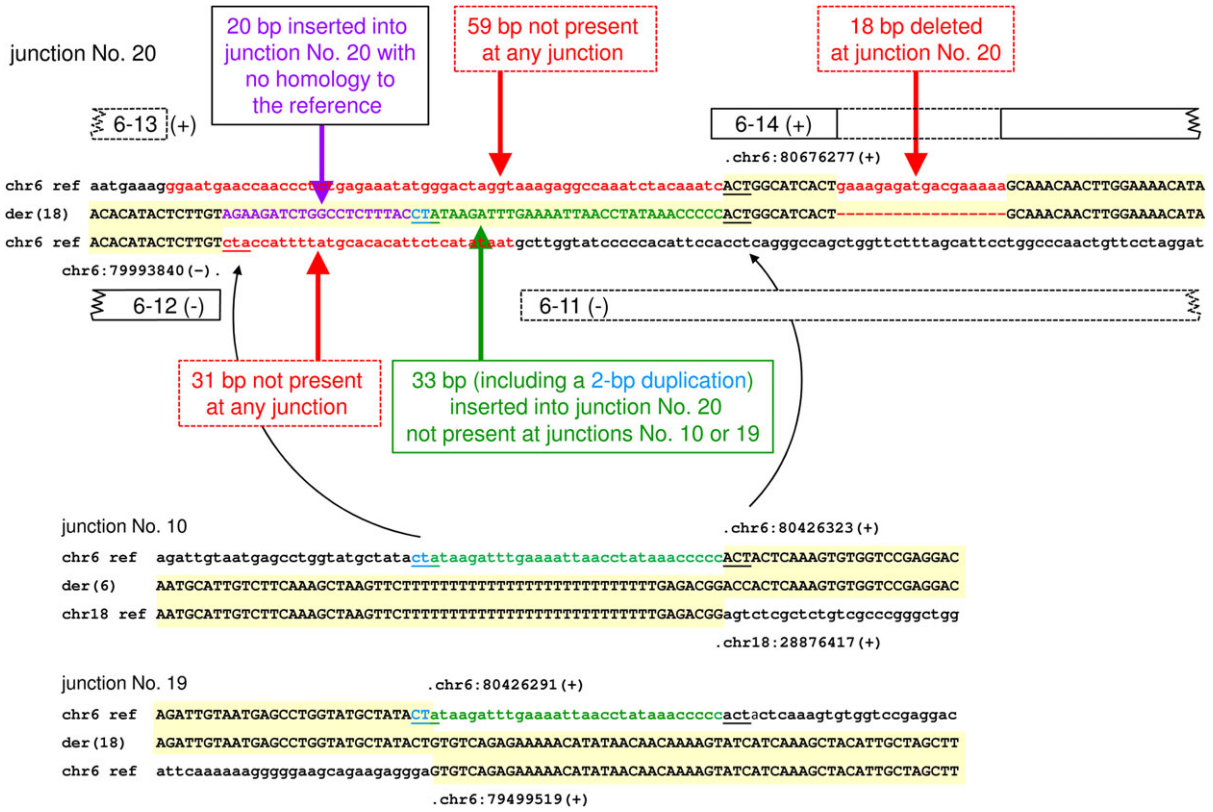

FIGURE 3 Nucleotide sequence of the highly complex junction No. 20. The sequences present at the junction are in capital letters and highlighted in yellow. Joined segments 6–12 and 6–14 (in head-to-head orientation) are indicated by solid rectangles, the original neighboring segments 6–11 and 6–13 are indicated by dashed rectangles. Deleted, moved, duplicated, and inserted DNA stretches are shown in red, green, blue, and violet, respectively. Sequences labeled "ref" and "der" show the reference sequences and sequences of the derivative chromosomes, respectively. Junctions No. 10 and 19, which both lack the 33 bp templated segment (inserted into junction No. 20), are shown for comparison. The microhomologies flanking the 33 bp segment and its insertion site are underlined and connected by curved arrows

absence of extended homology (low-copy repeats or repetitive elements) at the breakpoints, no microhomology (at seven junctions) or short microhomology of 1–6 bp (at 13 junctions), short deletions of 1–10 bp (at four junctions) and duplications of 2–4 bp (at three junctions). However, relatively larger deletions combined with microhomology (e.g., at junctions No. 1, 2, 8, 17, 18, and 20) can be typical of the more error-prone MMEJ mechanism (Seol et al., 2017). As NHEJ and MMEJ yield partly overlapping signatures at the junction sites, their role in the formation of individual breakpoint junctions cannot be unequivocally determined (Supp. Fig. S2). Microhomology is associated also with replication-based mechanisms (FoSTeS and MMBIR), which can also participate in CCRs caused by chromoanasynthesis (Liu et al., 2011), but other features of the CCR in our patient such as the absence of copy number gains and absence of microhomology at some junctions argue against their involvement.

Junction No. 20 is remarkable for deletions at the ends of both participating segments, insertion of a 33 bp DNA stretch from another breakpoint, insertion of 20 bp of DNA of unknown origin, and microhomologies of 3 bp flanking the 33 bp insertion (Fig. 3 and Supp. Table S1). We arbitrarily set the lower limit for a segment length to 1 kb and the shortest segments 6-3, 18-3 and 6–10 had the size of 2.2, 3.9, and 4.6 kb, respectively (Supp. Table S1). The presence of the "cut and paste" 33 bp DNA stretch with microhomology at both sides inserted into junction No. 20, which was only detected using Sanger sequencing, suggests that the repair machinery can recognize very small DNA fragments, which can be ligated into the final CCR. Indeed, a review of previously published chromothripsis events shows other instances of involvement of small segments (patients DGAP127 and UTR22 with 115–116 bp segments) (Collins et al., 2017; Redin et al., 2017). Accordingly, the chromosome shattering step is likely to produce DNA fragments ranging in length from base pairs to megabases, which are then reshuffled and incorporated into the derivative chromosomes, or, alternatively, are lost. Therefore, it cannot be excluded that other small deletions often seen at the CCR junctions including those in the present case might represent other short segments, which were lost or inserted elsewhere in the genome (where they could escape attention due to their small size, especially as insertional translocations, depending on the resolution of the sequencing technique used). Short deletions at the CCR junctions may thus reflect not just polishing of the fragment ends by repair enzymes, but closely placed double-strand breaks and loss of the intervening short fragments.

There is a continuous spectrum of human genetic variations ranging from 1 bp to many megabases. The size cut-off for SVs (currently rearrangements larger than 50 bp (Sudmant et al., 2015)) is changing with time and reflects the resolution of contemporary methods. Intuitively there might be a distinction between indels and SVs, possibly reflecting not primarily their absolute length but rather their mechanism

(small replication/repair errors for indels vs. chromosome segment reshuffling for SVs). The case of the 33 bp long fragment is interesting as it may be classified as an indel based on its length, but based on its mechanism it clearly belongs to classical SVs.

It has been shown that the repair of germline chromosomal shattering may involve a combination of different repair pathways. Our observations indicate that even very small fragments from shattered chromosomes are likely to be detected and handled by the repair machinery during germline chromothriptic chromosome reassembly.

ACKNOWLEDGMENTS

We thank Dustin Hancks for expert advice on retroposition, and the family of the patient for cooperation.

DISCLOSURE STATEMENT

The authors declare no conflict of interest.

ORCID


Zdenek Sedlacek http://orcid.org/0000-0001-6575-9163

REFERENCES

Arima, T., Drewell, R. A., Arney, K. L., Inoue, J., Makita, Y., Hata, A., … Surani, M. A. (2001). A conserved imprinting control region at the HYMAI/ZAC domain is implicated in transient neonatal diabetes mellitus. *Human Molecular Genetics*, *10*(14), 1475–1483.

Ashraf, T., Collinson, M. N., Fairhurst, J., Wang, R., Wilson, L. C., & Foulds, N. (2015). Two further patients with the 1q24 deletion syndrome expand the phenotype: A possible role for the miR199-214 cluster in the skeletal features of the condition. *American Journal of Medical Genetics Part A*, *167*(12), 3153–3160.

Bertelsen, B., Nazaryan-Petersen, L., Sun, W., Mehrjouy, M. M., Xie, G., Chen, W., … Tumer, Z. (2016). A germline chromothripsis event stably segregating in 11 individuals through three generations. *Genetics in Medicine*, *18*(5), 494–500.

Collins, R. L., Brand, H., Redin, C. E., Hanscom, C., Antolik, C., Stone, M. R., … Talkowski, M. E. (2017). Defining the diverse spectrum of inversions, complex structural variation, and chromothripsis in the morbid human genome. *Genome Biology*, *18*(1), 36.

De Gregori, M., Ciccone, R., Magini, P., Pramparo, T., Gimelli, S., Messa, J., … Zuffardi, O. (2007). Cryptic deletions are a common finding in "*balanced*," reciprocal and complex chromosome rearrangements: A study of 59 patients. *Journal of Medical Genetics*, *44*(12), 750–762.

de Ligt, J., Willemsen, M. H., van Bon, B. W., Kleefstra, T., Yntema, H. G., Kroes, T., … Vissers, L. E. (2012). Diagnostic exome sequencing in persons with severe intellectual disability. *New England Journal of Medicine*, *367*(20), 1921–1929.

de Pagter, M. S., van Roosmalen, M. J., Baas, A. F., Renkens, I., Duran, K. J., van Binsbergen, E., … Kloosterman, W. P. (2015). Chromothripsis in healthy individuals affects multiple protein-coding genes and can result in severe congenital abnormalities in offspring. *American Journal of Human Genetics*, *96*(4), 651–656.

Firth, H. V., Richards, S. M., Bevan, A. P., Clayton, S., Corpas, M., Rajan, D., … Carter, N. P. (2009). DECIPHER: Database of Chromosomal Imbalance and Phenotype in Humans Using Ensembl Resources. *American Journal of Human Genetics*, *84*(4), 524–533.

Freeze, H. H., Eklund, E. A., Ng, B. G., & Patterson, M. C. (2015). Neurological aspects of human glycosylation disorders. *Annual Review of Neuroscience*, *38*, 105–125.

Chatron, N., Haddad, V., Andrieux, J., Desir, J., Boute, O., Dieux, A., … Schluth-Bolard, C. (2015). Refinement of genotype-phenotype correlation in 18 patients carrying a 1q24q25 deletion. *American Journal of Medical Genetics Part A*, 167A(5), 1008–1017.

Chiang, C., Jacobsen, J. C., Ernst, C., Hanscom, C., Heilbut, A., Blumenthal, I., … Talkowski, M. E. (2012). Complex reorganization and predominant non-homologous repair following chromosomal breakage in karyotypically balanced germline rearrangements and transgenic integration. *Nature Genetics*, *44*(4), 390–397.

Kloosterman, W. P., Guryev, V., van Roosmalen, M., Duran, K. J., de Bruijn, E., Bakker, S. C., … Cuppen, E. (2011). Chromothripsis as a mechanism driving complex de novo structural rearrangements in the germline. *Human Molecular Genetics*, *20*(10), 1916–1924.

Kloosterman, W. P., Tavakoli-Yaraki, M., van Roosmalen, M. J., van Binsbergen, E., Renkens, I., Duran, K., … Cuppen, E. (2012). Constitutional chromothripsis rearrangements involve clustered double-stranded DNA breaks and nonhomologous repair mechanisms. *Cell Reports*, *1*(6), 648–655.

Li, H., & Durbin, R. (2009). Fast and accurate short read alignment with Burrows-Wheeler transform. *Bioinformatics*, *25*(14), 1754–1760.

Li, H., Handsaker, B., Wysoker, A., Fennell, T., Ruan, J., … Subgroup, G. P. D. P. (2009). The Sequence Alignment/Map format and SAMtools. *Bioinformatics*, *25*(16), 2078–2079.

Liu, P., Erez, A., Nagamani, S. C., Dhar, S. U., Kolodziejska, K. E., Dharmadhikari, A. V., … Bi, W. (2011). Chromosome catastrophes involve replication mechanisms generating complex genomic rearrangements. *Cell*, *146*(6), 889–903.

Lu, J., Helton, T. D., Blanpied, T. A., Racz, B., Newpher, T. M., Weinberg, R. J., & Ehlers, M. D. (2007). Postsynaptic positioning of endocytic zones and AMPA receptor cycling by physical coupling of dynamin-3 to Homer. *Neuron*, *55*(6), 874–889.

Ly, P., & Cleveland, D. W. (2017). Rebuilding chromosomes after catastrophe: Emerging mechanisms of chromothripsis. *Trends in Cell Biology*, *27*(12), 917–930.

Ly, P., Teitz, L. S., Kim, D. H., Shoshani, O., Skaletsky, H., Fachinetti, D., … Cleveland, D. W. (2017). Selective Y centromere inactivation triggers chromosome shattering in micronuclei and repair by non-homologous end joining. *Nature Cell Biology*, *19*(1), 68–75.

Middelkamp, S., van Heesch, S., Braat, A. K., de Ligt, J., van Iterson, M., Simonis, M., … Cuppen, E. (2017). Molecular dissection of germline chromothripsis in a developmental context using patient-derived iPS cells. *Genome Medicine*, *9*(1), 9.

Nazaryan-Petersen, L., Bertelsen, B., Bak, M., Jonson, L., Tommerup, N., Hancks, D. C., & Tumer, Z. (2016). Germline chromothripsis driven by L1-mediated retrotransposition and Alu/Alu homologous recombination. *Human Mutation*, *37*(4), 385–395.

Nazaryan-Petersen, L., & Tommerup, N. (2016). Chromothripsis and human genetic disease. In *eLS* (pp. 1–10). Chichester: John Wiley & Sons.

Pellestor, F., Anahory, T., Lefort, G., Puechberty, J., Liehr, T., Hedon, B., & Sarda, P. (2011). Complex chromosomal rearrangements: Origin and meiotic behavior. *Human Reproduction Update*, *17*(4), 476–494.

Pellestor, F., Gatinois, V., Puechberty, J., Genevieve, D., & Lefort, G. (2014). Chromothripsis: Potential origin in gametogenesis and preimplantation cell divisions. A review. *Fertility and Sterility*, *102*(6), 1785–1796.

Poot, M., & Haaf, T. (2015). Mechanisms of origin, phenotypic effects and diagnostic implications of complex chromosome rearrangements. *Molecular Syndromology*, *6*(3), 110–134.

Rausch, T., Zichner, T., Schlattl, A., Stutz, A. M., Benes, V., & Korbel, J. O. (2012). DELLY: Structural variant discovery by integrated paired-end and split-read analysis. *Bioinformatics*, *28*(18), i333–i339.

Redin, C., Brand, H., Collins, R. L., Kammin, T., Mitchell, E., Hodge, J. C., … Talkowski, M. E. (2017). The genomic landscape of balanced cytogenetic abnormalities associated with human congenital anomalies. *Nature Genetics*, *49*(1), 36–45.

Romeu, A., & Arola, L. (2014). Classical dynamin DNM1 and DNM3 genes attain maximum expression in the normal human central nervous system. *BMC Research Notes*, *7*, 188.

Seol, J. H., Shim, E. Y., & Lee, S. E. (2017). Microhomology-mediated end joining: Good, bad and ugly. *Mutation Research*, Jul 16. [Epub ahead of print].

Sfeir, A., & Symington, L. S. (2015). Microhomology-mediated end joining: A back-up survival mechanism or dedicated pathway? *Trends in Biochemical Sciences*, *40*(11), 701–714.

Sha, Z., Sha, L., Li, W., Dou, W., Shen, Y., Wu, L., & Xu, Q. (2015). Exome sequencing identifies SUCO mutations in mesial temporal lobe epilepsy. *Neuroscience Letters*, *591*, 149–154.

Shamseldin, H. E., Tulbah, M., Kurdi, W., Nemer, M., Alsahan, N., Al Mardawi, E., … Alkuraya, F. S. (2015). Identification of embryonic lethal genes in humans by autozygosity mapping and exome sequencing in consanguineous families. *Genome Biology*, *16*, 116.

Srivastava, S., Engels, H., Schanze, I., Cremer, K., Wieland, T., Menzel, M., … Naidu, S. (2016). Loss-of-function variants in HIVEP2 are a cause of intellectual disability. *European Journal of Human Genetics*, *24*(4), 556–561.

Stagi, S., Lapi, E., Pantaleo, M., Carella, M., Petracca, A., De Crescenzo, A., … de Martino, M. (2015). A new case of de novo 6q24.2-q25.2 deletion on paternal chromosome 6 with growth hormone deficiency: A twelve-year follow-up and literature review. *BMC Medical Genetics*, *16*, 69.

Steinfeld, H., Cho, M. T., Retterer, K., Person, R., Schaefer, G. B., Danylchuk, N., … Chung, W. K. (2016). Mutations in HIVEP2 are associated with developmental delay, intellectual disability, and dysmorphic features. *Neurogenetics*, *17*(3), 159–164.

Stephens, P. J., Greenman, C. D., Fu, B., Yang, F., Bignell, G. R., Mudie, L. J., … Campbell, P. J. (2011). Massive genomic rearrangement acquired in a single catastrophic event during cancer development. *Cell*, *144*(1), 27–40.

Sudmant, P. H., Rausch, T., Gardner, E. J., Handsaker, R. E., Abyzov, A., Huddleston, J., … Korbel, J. O. (2015). An integrated map of structural variation in 2,504 human genomes. *Nature*, *526*(7571), 75–81.

Varrault, A., Gueydan, C., Delalbre, A., Bellmann, A., Houssami, S., Aknin, C., … Journot, L. (2006). Zac1 regulates an imprinted gene network critically involved in the control of embryonic growth. *Developmental Cell*, *11*(5), 711–722.

Weckselblatt, B., Hermetz, K. E., & Rudd, M. K. (2015). Unbalanced translocations arise from diverse mutational mechanisms including chromothripsis. *Genome Research*, *25*(7), 937–947.

Weckselblatt, B., & Rudd, M. K. (2015). Human structural variation: Mechanisms of chromosome rearrangements. *Trends in Genetics*, *31*(10), 587–599.

Zeitouni, B., Boeva, V., Janoueix-Lerosey, I., Loeillet, S., Legoix-ne, P., Nicolas, A., … Barillot, E. (2010). SVDetect: A tool to identify genomic structural variations from paired-end and mate-pair sequencing data. *Bioinformatics*, *26*(15), 1895–1896.

SUPPORTING INFORMATION

Additional Supporting Information may be found online in the supporting information tab for this article.

How to cite this article: Slamova Z, Nazaryan-Petersen L, Mehrjouy MM, et al. Very short DNA segments can be detected and handled by the repair machinery during germline chromothriptic chromosome reassembly. *Human Mutation*. 2018; 1–8. https://doi.org/10.1002/humu.23408

MOLECULAR CYTOGENETICS

CASE REPORT Open Access

Anophthalmia, hearing loss, abnormal pituitary development and response to growth hormone therapy in three children with microdeletions of 14q22q23

Sophie Brisset[1,8†], Zuzana Slamova[2†], Petra Dusatkova[3†], Audrey Briand-Suleau[4,9], Karen Milcent[5,8], Corinne Metay[4,9], Martina Simandlova[2], Zdenek Sumnik[3], Lucie Tosca[1,7,8], Michel Goossens[4,9], Philippe Labrune[5,8], Elsa Zemankova[6], Jan Lebl[3], Gerard Tachdjian[1,7,8] and Zdenek Sedlacek[2*]

Abstract

Background: Microdeletions of 14q22q23 have been associated with eye abnormalities and pituitary defects. Other phenotypic features in deletion carriers including hearing loss and response to growth hormone therapy are less well recognized. We studied genotype and phenotype of three newly identified children with 14q22q23 deletions, two girls and one boy with bilateral anophthalmia, and compared them with previously published deletion patients and individuals with intragenic defects in genes residing in the region.

Results: The three deletions were *de novo* and ranged in size between 5.8 and 8.9 Mb. All three children lacked one copy of the *OTX2* gene and in one of them the deletion involved also the *BMP4* gene. All three patients presented partial conductive hearing loss which tended to improve with age. Analysis of endocrine and growth phenotypes showed undetectable anterior pituitary, growth hormone deficiency and progressive growth retardation in all three patients. Growth hormone therapy led to partial catch-up growth in two of the three patients but just prevented further height loss in the third.

Conclusions: The pituitary hypoplasia, growth hormone deficiency and growth retardation associated with 14q22q23 microdeletions are very remarkable, and the latter appears to have an atypical response to growth hormone therapy in some of the cases.

Keywords: Anophthalmia, 14q22q23 microdeletion, *OTX2*, Hearing loss, Pituitary, Growth hormone therapy

Background

The morphogenesis of midline brain structures, eyes, optic nerves and optic tracts is governed by a cascade of transcription factors including SOX2, OTX2 and BMP4 [1]. Congenital anophthalmia, which is among the most severe consequences of defects in this cascade, is often accompanied by pituitary dysfunction and growth failure due to growth hormone (GH) deficiency [2-6]. Mutations in *SOX2* are the most common cause of anophthalmia, and 10% of their carriers also show growth retardation [1]. The co-occurrence of eye malformations and GH deficiency is the highest (30%) in patients with *OTX2* mutations [3]. *BMP4* defects can induce a similar brain and ocular phenotype [6,7]. Mutations ranging from single nucleotide substitutions to cytogenetically visible deletions have been reported in *OTX2* and *BMP4*, which are both located in 14q22q23. We identified three unrelated patients with anophthalmia, partial hearing loss and pituitary defects due to microdeletions of this region. This gave us a unique opportunity to study not only the ocular phenotypes which are well associated with these rare genetic defects, but also other phenotypic features which are less well characterized.

* Correspondence: zdenek.sedlacek@lfmotol.cuni.cz
†Equal contributors
[2]Department of Biology and Medical Genetics, Charles University 2nd Faculty of Medicine and University Hospital Motol, Prague, Czech Republic
Full list of author information is available at the end of the article

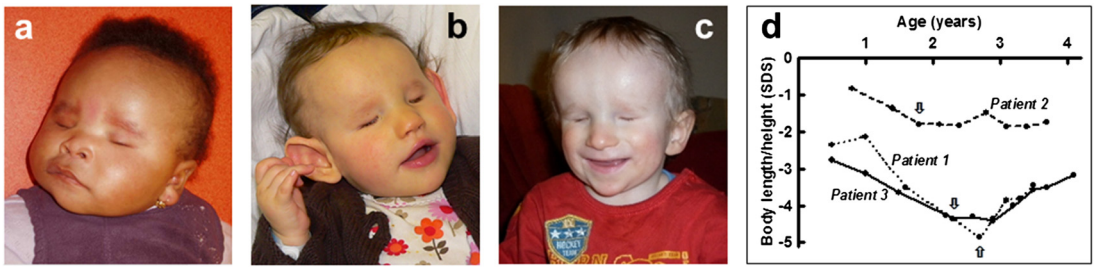

Figure 1 Facial photographs of the patients and their growth characteristics. (a) Patient 1 at the age of 6 months; **(b)** Patient 2 at the age of 7 months; **(c)** Patient 3 at the age of 22 months; **(d)** Development of body length with the onset of GH administration indicated by arrows.

Case presentation

Clinical reports

Patient 1

The girl (Figure 1a) was born to healthy parents of Mali origin at 38 weeks of gestation by Caesarean section because of abnormal fetal cardiac rhythm. Her birth weight, length and head circumference (HC) were 3,110 g (50th centile), 51 cm (75th centile), and 35.5 cm (75th centile), respectively. She showed bilateral anophthalmia. Brain magnetic resonance imaging (MRI) detected hypoplastic orbits, and absent optic nerves and optic chiasm. The anterior pituitary was undetectable, the posterior pituitary was ectopic with hypoplasia of the pituitary stalk, and the sella was small and flat. She had high forehead, microretrognathia, high arched palate, large ears, persistent hypotonia and right postaxial polydactyly. Cardiac examination revealed a systolic murmur and a perimembranous interventricular septal defect of 3 mm. Skeletal radiography and external genitalia were normal.

After birth, provoked otoacustic emissions were abnormal on the left side. Auditory evoked potentials at 3 years of age found a 60 dB threshold hearing in both ears. Because of persistent middle ear effusion, tympanostomic tubes were inserted, but had to be removed due to chronic otorrhea.

A very low serum IGF-I (9 μg/l) and cortisol (<10 nmol/l) levels at 10 days of life suggested GH deficiency and a cortisol function defect (confirmed by ACTH stimulation test). The levels of other pituitary hormones were normal (TSH 3.48 mUI/l, T4 17.8 pmol/l). The growth of Patient 1 progressively deteriorated from −2.4 SD (60 cm) at 6 months to −3.5 SD (71 cm) at 1.6 years and to −4.9 SD (75.5 cm) at 2.7 years of age (Figure 1d). GH therapy at a dose of 35 μg/kg/day initiated at the age of 2.7 years led to an improved growth rate and stepwise normalization of circulating IGF-I (4, 11 and 135 μg/l at the onset and after 3 and 12 months of therapy, respectively; normal age-specific serum IGF-I range is 51–218 μg/l).

Patient 2

The girl (Figure 1b) was born to healthy Czech parents in the 41st week of gestation with a weight of 3,500 g (50th centile), length of 52 cm (75th centile), and HC of 33 cm (10th centile). Bilateral anophthalmia and relative microcephaly were noted at birth. Brain MRI revealed absence of optic nerves, optic chiasm and optic tracts. The sella was flat, the pituitary stalk and posterior pituitary were present and normally located, but the anterior pituitary was undetectable. The patient showed profound hypotonia and very large, low-set dysplastic ears, high prominent forehead, high frontal hairline, and wide nose with horizontal nostrils, but no cardiac or genital defects. Radiography revealed the presence of 13 pairs of ribs and unpent arcs of vertebral corpus Th1.

Investigation of otoacustic emissions was not successful in the newborn. At 6 months of age she had normal hearing at the left side and moderate conductive hearing loss at the right side. Stenotic Eustachian tubes likely led to decreased pressure in the middle ear cavity. The hearing loss tended to improve with age.

Initially, the growth of the patient was normal. However, it started to decelerate to −0.8 SD (70 cm) at 10 months, −1.4 SD (76.3 cm) at 1.4 years and −1.8 SD (79 cm) at 1.8 years of age (Figure 1d). Endocrine assessment revealed GH deficiency (3.53 ug/l following insulin-induced hypoglycemia at 17 months of age) and IGF-I deficiency (11 ug/l; −1.79 SD) but normal other pituitary functions (TSH 1.19 mIU/l, fT4 12.2 pmol/l, FSH 8.9 IU/l, LH 0.9 IU/l, cortisol 555 nmol/l, prolactin 4.7 ug/l). GH therapy at a dose of 25 μg/kg/day was initiated at the age of 1.8 years. It improved the growth rate and the serum IGF-I level (5, 75 and 116 μg/l at the onset, 12 and 24 months of therapy, respectively) but did not lead to catch-up growth (99 cm at 4 years, i.e. -1.5 SD, Figure 1d).

Patient 3

The boy (Figure 1c) was born to healthy Czech parents in the 37th week of gestation by Caesarean section due to intrauterine growth retardation with a weight of

2,060 g and length of 44 cm (both below the 3rd centile for the gestational age), bilateral anophthalmia and marked hypotonia. Brain MRI revealed absent optic chiasm; however, extraocular muscles were preserved. Similarly to Patient 2, the sella was flat, the pituitary stalk and posterior pituitary were present and normally located, but the anterior pituitary was undetectable. Patient 3 showed mesocephaly with prominent narrow forehead, a small narrow face and a wide nasal bridge. He had no apparent morphological ear abnormalities and no cardiac, spinal, abdominal, or genital defects. His bilateral testicular retention required surgical management.

In the neonatal period, the investigation of otoacustic emissions was unsuccessful. At the age of 3 months he showed mild hearing loss of the right ear and medium hearing loss of the left ear. Despite the tympanometry was normal, the hearing loss was apparently conductive due to stenotic ear canals. Also in this patient hearing gradually improved with age.

Intrauterine growth retardation was followed by severe postnatal growth failure: at the age of 7 weeks the boy had a length of 48.4 cm (−3.7 SD), and weight of 3,010 g, and his growth had further deteriorated (Figure 1d). He suffered from GH deficiency (1.79 ug/l following clonidine stimulation at 2.3 years of age) and IGF-I deficiency (2 ug/l). Other pituitary functions were apparently normal (TSH 2.75 mIU/l, fT4 11.8 pmol/l, FSH 0.48 IU/l, LH 0.07 IU/l, cortisol 201 nmol/l, prolactin 5.7 ug/l); however, the bilateral testicular retention might be suggestive of a gonadotropin deficiency. GH therapy at a dose of 25 μg/kg/day was initiated at the age of 2.3 years. His height velocity on therapy was atypical, with only a moderate increase within the first year of GH administration but a marked increase thereafter (92.0 cm at 4.1 years, i. e. -3.17 SD, Figure 1d). Serum IGF-I levels were gradually increasing to 6, 19, 33, 56 and 67 μg/l at the onset and during the first two years of therapy.

Laboratory methods

The study was approved by the local ethics committees and all analyses were performed after proper informed consent. Karyotyping of the patients was performed using standard methods. Array comparative genomic hybridization (CGH) used 180K and 105K CGH arrays (Agilent Technologies) in Patient 1 and Patients 2/3, respectively. The deletions were confirmed in the patients and tested in the parents using fluorescence in situ hybridization (FISH) with probes RP11-533L7/RP11-550 M19 and RP11-550M19 (BlueGnome) in Patients 1 and 2, respectively. In Patient 3 the deletion was confirmed using a 60K CGH array (Agilent Technologies).

Results

Karyotyping did not show chromosome abnormalities in any of the three patients. Array CGH revealed interstitial deletions of 14q22q23 of varying size (Figure 2) in the absence of additional relevant submicroscopic aberrations. Patient 1 carried an 8.8 Mb long deletion (chr14:50293781–

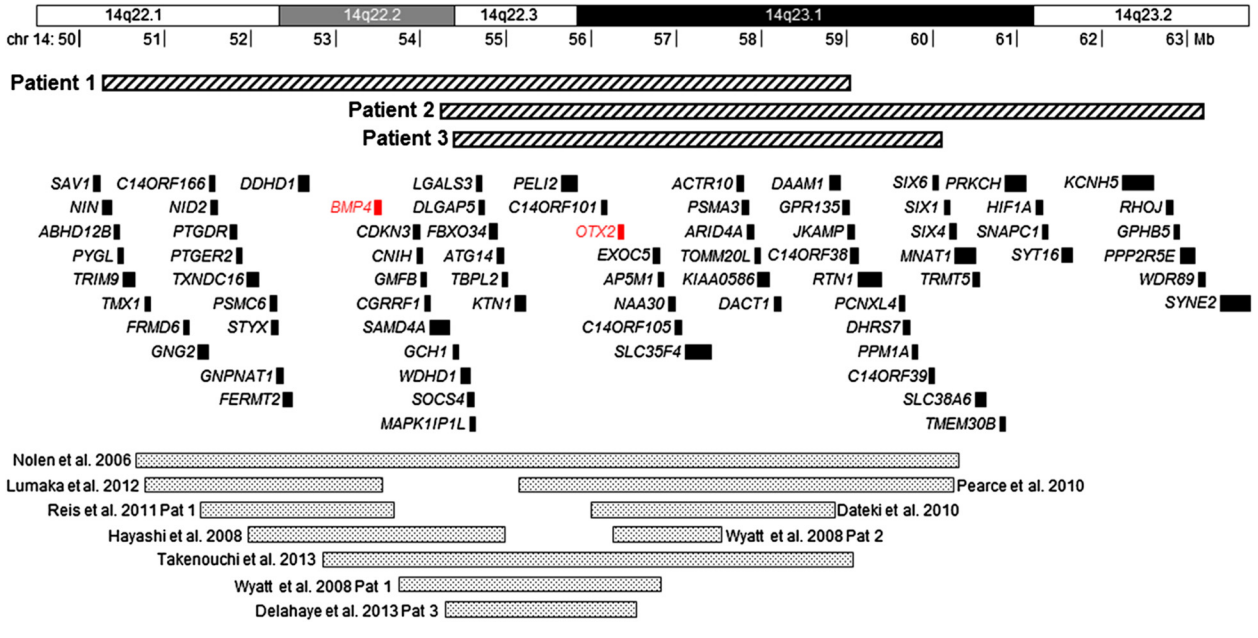

Figure 2 Schematic representation of the 14q22q23 region affected by deletions in the patients. The deletions in our patients are shown as thick hatched bars, the deletions overlapping *OTX2* and/or *BMP4* in published cases as dotted bars. Intragenic deletions in *OTX2* or *BMP4* are not shown. Protein-coding genes are indicated by black rectangles (*OTX2* or *BMP4* are in red). The chromosome 14 banding pattern and megabase scale are also included.

59068634, hg18) removing multiple genes including *BMP4* and *OTX2* but not the *SIX* gene cluster. Patient 2 had a deletion of 8.9 Mb (chr14:54251697–63177878) affecting *OTX2* and the *SIX* gene cluster. Patient 3 had a 5.8 Mb long deletion (chr14:54431790–60167626) removing *OTX2* and a part of the *SIX* gene cluster. Using independent methods, all deletions were confirmed in the patients but not in any of the parents, thus indicating the *de novo* nature of the aberrations.

Discussion

We present a case series of three patients with bilateral anophthalmia caused by microdeletions of 14q22q23. Their phenotype was further characterized by hearing impairment, abnormal pituitary development leading to GH deficiency and early growth failure, and dysmorphic facial features. The overview of phenotypes observed in published cases with 14q22q23 deletions and in our three patients is in Table 1.

The 14q22q23 region is critical for eye and pituitary development. Anophthalmia and other ocular anomalies were associated with heterozygous defects in *OTX2* [3,8,9] or *BMP4* [7,10,11], and also with deletions involving both these genes [4,6,12]. While *OTX2* was deleted in all our patients, *BMP4* was deleted only in Patient 1 (Figure 2). Nevertheless, the ocular phenotype was similar in all three children. The phenotypic effect of *OTX2* and *BMP4* disruptions is very variable ranging between anophthalmia/microphthalmia, corneal opacity and no abnormality at all, even in family members with the same mutation [2,5,9-13], and the phenotype does not have to be more severe in patients with combined *OTX2*/*BMP4* defects [4,12]. Patients 2 and 3 also lacked *SIX6*; however, defects of this candidate gene have not been identified in anophthalmia [1].

All three patients suffered from transient partial conductive hearing loss. Previous reports of patients with 14q22q23 deletions were inconsistent, varying from not mentioning the hearing status over normal function [7,12] to severe unilateral hearing loss [4,9], indicating very variable expressivity. We speculate that skeletal abnormalities of the facial-cranial junction of the skull associated with anophthalmia due to the *OTX2* defect can induce stenosis of ear canals and/or Eustachian tubes and hearing impairment. Changing proportions of these structures during growth could also explain the gradual improvement of hearing with age observed in our patients. Interestingly, Patient 2 with large low-set dysplastic ears was the only our patient with *SIX1* disruption. Homozygous knockout of this gene in mice causes malformations of the auditory system including outer ears [14]. Deletions in two published patients also involved *SIX1* and were associated with malformed ears, although differently from Patient 2 [4,9]. *OTX2* defects themselves could also contribute to ear anomalies [15].

Our patients showed abnormal pituitary development, GH deficiency and growth retardation. Normal birth parameters and postnatal growth failure similar to that in Patients 1 and 2 were reported in some cases with 14q22q23 deletions [3,4,11,12]. On the other hand, Patient 3 suffered from severe intrauterine growth retardation without postnatal catch-up. An improvement of growth was evident after GH therapy in all our patients although the response varied. In Patients 1 and 3 the therapy induced an increase of growth velocity and improvement of their height, whereas in Patient 2 it just prevented further growth deterioration. However, in Patient 2 the growth failure was least pronounced with height of −1.8 SD at the start of the GH therapy, and this fact could influence the GH response. Similarly, two published 14q22q23 deletion patients treated with GH remained with their height at −2 SD after five and three years of therapy [4,13], and the height of a boy with a missense *OTX2* mutation remained at −2.3 SD after eight years of therapy [2]. As no reports are currently available on final height of 14q22q23 deletion patients, it remains to be seen if Patients 1 and 3 correct their growth failure completely or if they just reach the current height range of Patient 2. Differences in the deleted genes do not offer an obvious explanation for the differences in responsiveness to the GH therapy. Two genes involved in pituitary development, *OTX2* and *SIX6*, were disrupted in Patients 2 and 3. Patient 1 had a deletion of *OTX2* and *BMP4*, but not of *SIX6*. The differences in pituitary morphology between Patient 1 and Patients 2 and 3 can also be attributed solely to the variability seen among carriers of isolated *OTX2* defects [1,3].

Finally, polydactyly was present in Patient 1 with a deletion of *BMP4*. This gene plays an important role in the onset of endochondral bone formation in humans, and its mutations were associated with polysyndactyly [4,11].

Recently, two papers were published describing patients with deletions overlapping the proximal and distal part of the 14q22q23 region [16,17]. A family with Frias syndrome carried a deletion of 14q22.1q22.3 spanning the interval between *GNG2* and *KTN1*, with *BMP4* haploinsufficiency being likely responsible for the phenotype which included hypoplasia of corpus callosum, minor ocular anomalies, specific tooth defects, digit anomalies, short stature and intellectual impairment [16]. The other deletion involving 14q22.3q23.2 and extending from *PSMA3* over the *SIX* cluster to *SYNE2* was identified in a patient with facial dysmorphism, choanal atresia, esophageal reflux, defects of hands and feet, seizures and intellectual disability [17]. Interestingly, in the latter case neither microphthalmia/anophthalmia nor pituitary anomalies were present (MRI was normal), and neither *OTX2*

Table 1 Clinical features in eighteen patients with 14q22q23 deletions

Report	Nolen et al. [4]	Hayashi et al. [11]	Bakrania et al. [6]	Bakrania et al. [6]	Wyatt et al. [8]	Wyatt et al. [8]	Dateki et al. [3]	Reis et al. [7]	Delahaye et al. [13]	Lumaka et al. [10]	Lumaka et al. [10]	Lumaka et al. [10]	Lumaka et al. [10]	Pearce et al. [9]	Takenouchi et al. [12]	Present study	Present study	Present study
Patient no.	1	1	1	2	1	2	5	1	3	I-1	II-2	III-5	III-6	1	1	1	2	3
14q deletion	q22.1 q23.1	q22.1 q23.1	q22.3 q23.2	q22.2 q23.1	q22.2 q22.3	q22.3 q23.1	q22.3 q23.1	q22.1 q22.2	q22.2 q23.1	q22.1 q22.2	q22.1 q22.2	q22.1 q22.2	q22.1 q22.2	q22.3 q23.1	q22.2 q23.1	q22.1 q23.1	q22.3 q23.2	q22.3 q23.1
Sex	M	F	F	M	F	F	M	F	M	M	F	F	F	F	F	F	F	M
Age at last examination	5 yr	18 mo	N.D.	N.D.	19 mo	3 yr	2 yr	6 yr	24 yr	Adult	Adult	13 mo	11 mo	4 mo	3 yr	4 yr	4 yr	4 yr
Anophthamia unilateral (AOU)/ bilateral (AOB); microphthalmia unilateral (MOU)/ bilateral (MOB)	AOB	-	AOB	AOB	MOB	AOB	AOU/ MOU	MOB	MOB	-	-	-	MOB	AOU/ MOU	MOB	AOB	AOB	AOB
Optic nerve and/or chiasma and/or optic tracts hypoplasia/ agenesis	+	-	+	+	N.D.	N.D.	N.D.	-	N.D.	-	-	-	N.D.	+	-	+	+	+
Cerebral and/or facial midline defects	+	-	+	+	-	-	-	-	+	-	-	+	+	+	-	+	-	-
Pituitary aplasia/ hypoplasia	+	-	N.D.	+	-	-	+	-	N.D.	N.D.	N.D.	N.D.	N.D.	-	-	+	+	+
Hormonal deficiencies: growth hormone deficiency (GHD)/ hypothyroidism (HT)	GHD	N.D.	HT[#]	-	N.D.	N.D.	GHD	N.D.	N.D.	N.D.	N.D.	-	N.D.	-	-	GHD	GHD	GHD
Prenatal growth	Normal	Normal	N.D.	N.D.	Normal	Normal	Normal	Normal	N.D.	Normal	Normal	Retarded	Retarded	Normal	Normal	Normal	Normal	Retarded
Postnatal growth	Retarded	Retarded	N.D.	N. D.	N.D.	N.D.	Retarded	Retarded	N.D.	Normal	Retarded	Retarded	Retarded	N.A.*	Normal	Retarded	Retarded	Retarded
Microcephaly	+	-	-	+	-	-	+	-	+	-	-	-	+	+	-	-	+	-
Hearing loss/ ear anomalies	+	-	-	+	-	-	N.D.	-	-	-	-	+	-	+	-	+	+	+
Undescended testes	+	N.A.	N.A.	+	N.A.	N.A.	N.D.	N.A.	-	-	N.A.	N.A.	N.A.	N.A.	N.A.	N.A.	N.A.	+
Developmental delay/intellectual disability	+	+	+	+	-	+	+	+	+	-	-	+	+	N.A.*	+	+	+	+

Table 1 Clinical features in eighteen patients with 14q22q23 deletions *(Continued)*

Polydactyly/ syndactyly	+	+	-	-	-	-	-	-	-	+	+	-	+	-	-	+	-	-
Major additional extracranial symptoms								SHORT syndrome; partial lipodystrophy	Renal			-		Duodenal atresia	Profound hypotonia			

N.D., not described; N.A., not applicable; *patient too young; #not specified if secondary (central) or primary (peripheral).
Similarly to Figure 2, this table does not list patients with deletions assessed using karyotyping in whom the genes affected are uncertain and small deletions affecting only *OTX2* or *BMP4* exons. The deletions in patients described by Bakrania et al., 2008 were identified using karyotyping and MLPA analysis was used to show that both deletions affected both *OTX2* and *BMP4*.

nor *BMP4* were deleted. These papers further illustrate the intra- and interfamilial variability which, together with biased and incomplete reporting of the phenotypes, complicates the genotype-phenotype correlation in patients with unique deletions affecting multiple genes which participate in different molecular pathways [16,17].

Conclusions

Our case series study of three patients with deletions of 14q22q23 demonstrated the phenotypic features and variable expressivity of this genetic defect. Comparison with previously published patients with similar microdeletions and mutations in the *OTX2* gene suggests that most symptoms presented by affected patients could be attributed to *OTX2* haploinsufficiency. Growth retardation due to GH deficiency is very remarkable in these patients and GH treatment can increase the growth velocity especially in the most severe cases but the response can be atypical. The hearing impairment can be transient and improves with age.

Consent

Written informed consent was obtained from the parents of the patients for publication of this report and the accompanying images. A copy of the written consent is available for review by the Editor-in-Chief of this journal.

Competing interests

The authors declare that they have no competing interests.

Authors' contributions

SB, ZSl, PD, ABS, CM, LT and MG carried out the cytogenetic and molecular cytogenetic studies; JL, ZSu, MS, EZ, SB, CM, KM and PL participated in the analysis of the phenotype and genetic counseling; PD, ZSe, JL and SB drafted the manuscript; ZSu edited the manuscript; ZSe, JL and GT conceived, designed and coordinated the study. All authors read and approved the final manuscript.

Acknowledgments

We thank the families for their cooperation. This work was supported by Direction de l'Hospitalisation et de l'Organisation des Soins, grants NT13692 and DRO UH Motol 00064203 from the Czech Ministry of Health, and CZ.2.16/3.1.00/24022.

Author details

[1]AP-HP, Service d'Histologie Embryologie et Cytogénétique, Hôpital Antoine Béclère, Clamart, France. [2]Department of Biology and Medical Genetics, Charles University 2nd Faculty of Medicine and University Hospital Motol, Prague, Czech Republic. [3]Department of Pediatrics, Charles University 2nd Faculty of Medicine and University Hospital Motol, Prague, Czech Republic. [4]AP-HP, Service de Biochimie-Génétique, Plateforme de Génétique Constitutionnelle, Hôpital Henri Mondor, Créteil, France. [5]AP-HP, Service de Pédiatrie, Hôpital Antoine Béclère, Clamart, France. [6]Genetic and Pediatric Ambulance, Benesov, Czech Republic. [7]INSERM U935, Villejuif, France. [8]Université Paris-Sud, Faculté de Médecine Paris-Sud, Le Kremlin Bicêtre, France. [9]INSERM U955, Université Paris 12, Créteil, France.

Received: 10 December 2013 Accepted: 18 February 2014
Published: 28 February 2014

References

1. Slavotinek AM: **Eye development genes and known syndromes.** *Mol Genet Metab* 2011, **104:**448–456.
2. Ashkenazi-Hoffnung L, Lebenthal Y, Wyatt AW, Ragge NK, Dateki S, Fukami M, Ogata T, Phillip M, Gat-Yablonski G: **A novel loss-of-function mutation in OTX2 in a patient with anophthalmia and isolated growth hormone deficiency.** *Hum Genet* 2010, **127:**721–729.
3. Dateki S, Kosaka K, Hasegawa K, Tanaka H, Azuma N, Yokoya S, Muroya K, Adachi M, Tajima T, Motomura K, Kinoshita E, Moriuchi H, Sato N, Fukami M, Ogata T: **Heterozygous orthodenticle homeobox 2 mutations are associated with variable pituitary phenotype.** *J Clin Endocrinol Metab* 2010, **95:**756–764.
4. Nolen LD, Amor D, Haywood A, St Heaps L, Willcock C, Mihelec M, Tam P, Billson F, Grigg J, Peters G, Jamieson RV: **Deletion at 14q22-23 indicates a contiguous gene syndrome comprising anophthalmia, pituitary hypoplasia, and ear anomalies.** *Am J Med Genet A* 2006, **140:**1711–1718.
5. Schilter KF, Schneider A, Bardakjian T, Soucy JF, Tyler RC, Reis LM, Semina EV: **OTX2 microphthalmia syndrome: four novel mutations and delineation of a phenotype.** *Clin Genet* 2011, **79:**158–168.
6. Bakrania P, Efthymiou M, Klein JC, Salt A, Bunyan DJ, Wyatt A, Ponting CP, Martin A, Williams S, Lindley V, Gilmore J, Restori M, Robson AG, Neveu MM, Holder GE, Collin JR, Robinson DO, Farndon P, Johansen-Berg H, Gerrelli D, Ragge NK: **Mutations in BMP4 cause eye, brain, and digit developmental anomalies: overlap between the BMP4 and hedgehog signaling pathways.** *Am J Hum Genet* 2008, **82:**304–319.
7. Reis LM, Tyler RC, Schilter KF, Abdul-Rahman O, Innis JW, Kozel BA, Schneider AS, Bardakjian TM, Lose EJ, Martin DM, Broeckel U, Semina EV: **BMP4 loss-of-function mutations in developmental eye disorders including SHORT syndrome.** *Hum Genet* 2011, **130:**495–504.
8. Wyatt A, Bakrania P, Bunyan DJ, Osborne RJ, Crolla JA, Salt A, Ayuso C, Newbury-Ecob R, Abou-Rayyah Y, Collin JR, Robinson D, Ragge N: **Novel heterozygous OTX2 mutations and whole gene deletions in anophthalmia, microphthalmia and coloboma.** *Hum Mutat* 2008, **29:**E278–E283.
9. Pearce ZD, Droste PJ, Aaberg TM Jr, Hassan AS: **Ophthalmic and systemic findings in interstitial deletions of chromosome 14q: a case report and literature review.** *Ophthalmic Genet* 2012, **33:**161–166.
10. Lumaka A, Van Hole C, Casteels I, Ortibus E, De Wolf V, Vermeesch JR, Lukusa T, Devriendt K: **Variability in expression of a familial 2.79 Mb microdeletion in chromosome 14q22.1-22.2.** *Am J Med Genet A* 2012, **158A:**1381–1387.
11. Hayashi S, Okamoto N, Makita Y, Hata A, Imoto I, Inazawa J: **Heterozygous deletion at 14q22.1-q22.3 including the BMP4 gene in a patient with psychomotor retardation, congenital corneal opacity and feet polysyndactyly.** *Am J Med Genet A* 2008, **146A:**2905–2910.
12. Takenouchi T, Nishina S, Kosaki R, Torii C, Furukawa R, Takahashi T, Kosaki K: **Concurrent deletion of BMP4 and OTX2 genes, two master genes in ophthalmogenesis.** *Eur J Med Genet* 2013, **56:**50–53.
13. Delahaye A, Bitoun P, Drunat S, Gerard-Blanluet M, Chassaing N, Toutain A, Verloes A, Gatelais F, Legendre M, Faivre L, Passemard S, Aboura A, Kaltenbach S, Quentin S, Dupont C, Tabet AC, Amselem S, Elion J, Gressens P, Pipiras E, Benzacken B: **Genomic imbalances detected by array-CGH in patients with syndromal ocular developmental anomalies.** *Eur J Hum Genet* 2012, **20:**527–533.
14. Zheng W, Huang L, Wei ZB, Silvius D, Tang B, Xu PX: **The role of Six1 in mammalian auditory system development.** *Development* 2003, **130:**3989–4000.
15. Chassaing N, Sorrentino S, Davis EE, Martin-Coignard D, Iacovelli A, Paznekas W, Webb BD, Faye-Petersen O, Encha-Razavi F, Lequeux L, Vigouroux A, Yesilyurt A, Boyadjiev SA, Kayserili H, Loget P, Carles D, Sergi C, Puvabanditsin S, Chen CP, Etchevers HC, Katsanis N, Mercer CL, Calvas P, Jabs EW: **OTX2 mutations contribute to the otocephaly-dysgnathia complex.** *J Med Genet* 2012, **49:**373–379.
16. Martinez-Fernandez ML, Bermejo-Sanchez E, Fernandez B, Macdonald A, Fernandez-Toral J, Martinez-Frias ML: **Haploinsufficiency of BMP4 gene may be the underlying cause of Frias syndrome.** *Am J Med Genet A* 2014, **164:**338–345.
17. Martinez-Frias ML, Ocejo-Vinyals JG, Arteaga R, Martinez-Fernandez ML, Macdonald A, Perez-Belmonte E, Bermejo-Sanchez E, Martinez S: **Interstitial deletion 14q22.3-q23.2: genotype-phenotype correlation.** *Am J Med Genet A* 2014. in press.

doi:10.1186/1755-8166-7-17
Cite this article as: Brisset *et al.*: Anophthalmia, hearing loss, abnormal pituitary development and response to growth hormone therapy in three children with microdeletions of 14q22q23. *Molecular Cytogenetics* 2014 **7**:17.

Case Report

Cytogenetic and Genome Research

Cytogenet Genome Res 2012;136:15–20
DOI: 10.1159/000334709

Accepted: August 29, 2011
by M. Schmid
Published online: December 8, 2011

Mechanism and Genotype-Phenotype Correlation of Two Proximal 6q Deletions Characterized Using mBAND, FISH, Array CGH, and DNA Sequencing

M. Vlckova[a] M. Trkova[b] Z. Zemanova[c] M. Hancarova[a] D. Novotna[a] D. Raskova[b] A. Puchmajerova[a] J. Drabova[a] Z. Zmitkova[a] Y. Tan[a] Z. Sedlacek[a]

[a]Department of Biology and Medical Genetics, Charles University 2nd Faculty of Medicine and University Hospital Motol, [b]Gennet, and [c]Center of Oncocytogenetics, Institute of Clinical Biochemistry and Laboratory Diagnostics, Charles University 1st Faculty of Medicine and General University Hospital, Prague, Czech Republic

Key Words
Array CGH · Centromere fission · Deletion junction · Marker chromosome · Proximal 6q deletion

Abstract
Proximal 6q deletions have a milder phenotype than middle and distal 6q deletions. We describe 2 patients with non-overlapping deletions of about 15 and 19 Mb, respectively, which subdivide the proximal 6q region into 2 parts. The aberrations were identified using karyotyping and analysed using mBAND and array CGH. The unaffected mother of the first patient carried a mosaic karyotype with the deletion in all metaphases analysed and a small supernumerary marker formed by the deleted material in about 77% of cells. Her chromosome 6 centromeric signal was split between the deleted chromosome and the marker, suggesting that this deletion arose through the centromere fission mechanism. In this family the location of the proximal breakpoint in the centromere prevented cloning of the deletion junction, but the junction of the more distal deletion in the second patient was cloned and sequenced. This analysis showed that the latter aberration was most likely caused by non-homologous end joining. The second patient also had a remarkably more severe phenotype which could indicate a partial overlap of his deletion with the middle 6q interval. The phenotypes of both patients could be partly correlated with the gene content of their deletions and with phenotypes of other published patients.

Three different phenotypic groups have been suggested in carriers of interstitial 6q deletions according to the location of the defect: proximal deletions (6q11q16) with upslanted fissures, thin lips, and hernias; middle deletions (6q15q25) with microcephaly, hypertelorism, intrauterine growth retardation, respiratory problems, and limb malformations; and distal deletions (6q25qter) with cleft palate, retinal abnormalities, genital hypoplasia, and seizures [Hopkin et al., 1997]. Hypotonia, ear and facial dysmorphism, and mental retardation are common to all 3 groups [Hopkin et al., 1997]. However, most of the older studies were based solely on karyotyping, and the size and location of the deletions were determined only at low resolution. The recent boom of microarray methods allows fine mapping of the deletion breakpoints and a much more precise delineation of the extent and gene content

KARGER

Fax +41 61 306 12 34
E-Mail karger@karger.ch
www.karger.com

1424–8581/12/1361–0015$38.00/0

Accessible online at:
www.karger.com/cgr

Zdenek Sedlacek
Department of Biology and Medical Genetics
Charles University 2nd Faculty of Medicine and University Hospital Motol
Plzenska 130/221, CZ–15000 Prague 5 (Czech Republic)
Tel. +420 257 296 153, E-Mail zdenek.sedlacek@lfmotol.cuni.cz

of the aberrations which in turn allows better genotype-phenotype correlations. In addition, molecular analysis of the deletion breakpoints can shed light on the aberration mechanisms.

We present 2 patients with proximal 6q deletions identified using karyotyping. Detailed analysis of the deletions showed that they subdivided the proximal 6q region into 2 parts of similar size. One of the deletions involved the centromere and arose most likely through the centromere fission mechanism, while the second deletion was probably caused by non-homologous end joining. The patients had remarkably different phenotypes which could be partly correlated with the gene content of their deletions and with phenotypes of other patients with proximal 6q deletions.

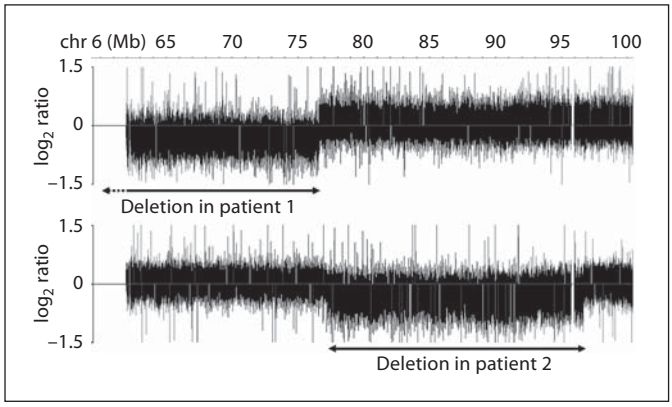

Fig. 1. Fine mapping of deletions in patients 1 and 2 using array CGH. The deletions are marked by double arrows. In patient 1 the proximal breakpoint mapped to the centromere gap and the exact size of the deletion was not known (dashed arrow). The deletions did not overlap and were separated by about 0.7 Mb of DNA.

Materials and Methods

Case Report

Patient 1 was the second child of healthy unrelated parents. The age of the mother and father was 41 and 45 years, respectively. The pregnancy was uneventful. Cytogenetic analysis of amniotic fluid cells performed due to advanced maternal age showed an apparently normal female karyotype. The delivery was at the 31st week of gestation by Caesarean section due to breech and fetal distress. The birth weight of the girl was 1,740 g (>75th centile) and length was 44 cm (>75th centile). The neonatal period was unremarkable. At the age of 2 months she developed hypotonia and affective paroxysms. EEG showed an abnormal pattern, and subsequent MRI proved delayed myelinization and bilateral frontal lobe atrophy, but no other major anomalies. The girl was referred to a geneticist at the age of 3 years because of developmental delay and absent speech. She had mild facial dysmorphism (high forehead, hypertelorism, epicanthal folds, dysplastic ears), single palmar crease on the right hand, pectus excavatum, hypotonia, and mild mental retardation. The audiologic exam was normal.

Patient 2 was the first child of healthy unrelated 30-year-old parents. Fetal ultrasound showed a heart defect and cleft palate. Prenatal karyotype was 46,XY,?del(6)(q?). During the third trimester, polyhydramnion occurred. The boy was born at the 40th week of gestation by spontaneous delivery. His weight was 3,390 g (>50th centile) and length was 53 cm (>95th centile). He suffered from a congenital heart defect (common atrium), cleft palate, and diaphragmatic hernia. Facial dysmorphism (low forehead, epicanthal folds, prominent eyelids, broad nasal tip, anteverted flared nostrils, long philtrum, micrognathia, dysplastic ears), atypical dermatoglyphs, micropenis, and cryptorchidism were also present. On examination at the age of 8 months his length was 74 cm (>50th centile), weight was 8,720 g (25th centile), and head circumference was 48 cm (95th centile). The boy suffered from developmental delay, seizures, laryngomalacia, bilateral iris coloboma and optic disc hypoplasia, and showed hypermobility of joints. EEG proved focal epilepsy, and CT scan showed global atrophy of the brain, partial agenesis of corpus callosum, and dilatation of the ventricles.

Karyotyping, Array CGH, mBAND, FISH, and Molecular Analysis of the Breakpoints

Cytogenetic analysis of blood lymphocytes was performed using standard protocols. mBAND analysis with the XCyte6 probe (MetaSystems, Altlußheim, Germany) was used for fine assessment of the deletions in both patients. Chromosome 6 painting probe WCP6 (Cambio, Cambridge, UK) was used to exclude a balanced insertional translocation in the parents of patient 2. FISH analysis of patient 1 and her mother was performed with chromosome 6 centromeric probe D6Z1 (Cytocell, Cambridge, UK). Genomic DNA was isolated from blood using Gentra Puregene Blood Kit (Qiagen, Hilden, Germany). Custom array CGH analysis was performed by Nimblegen on the catalogue array HG18_CHR6_FT with median probe spacing of 404 bp, and the results were analysed using SignalMap (Nimblegen, Madison, Wisc., USA). Long-range PCR (LR-PCR) used the Expand Long Template PCR System (Roche, Basel, Switzerland). The primer sequences are available on request. PCR fragments were purified using QIAamp PCR Purification Kit (Qiagen) and sequenced on an ABI PRISM 3100 automatic sequencer (Applied Biosystems, Foster City, Calif., USA). Bioinformatic analysis used the hg18 human genome assembly available in the UCSC Genome Browser (http://genome.ucsc.edu/cgi-bin/hgGateway).

Results

Karyotyping of patient 1 showed a small deletion of 6q11q13. Array CGH mapped the proximal deletion breakpoint to the centromere genome assembly gap (chr 6 Mb 58.89–61.94). The distal breakpoint mapped around Mb 76.55. The total size of the deleted region was ~15 Mb (fig. 1). It contained 34 protein-coding RefSeq genes. The unaffected mother of patient 1 carried a mosaic karyo-

type with the same deletion in all metaphases analysed and, in addition, a small supernumerary marker in 77% of cells, probably a ring chromosome. mBAND analysis confirmed that the marker chromosome constituted of proximal 6q material deleted from the derived chromosome 6 (fig. 2A).

Postnatal cytogenetic analysis of patient 2 revealed a deletion of 6q14q16, and mBAND analysis confirmed the result of the karyotyping (fig. 2B). Chromosome painting excluded a balanced insertional translocation in both parents who had normal karyotypes. Array CGH analysis of patient 2 indicated that the deletion affected chromosome 6 between Mb 77.23–96.63. The length of the deletion was ~19.5 Mb (fig. 1). The deleted region contained 58 protein-coding RefSeq genes.

FISH analysis of the mother of patient 1 with the chromosome 6 centromeric probe showed in all cells analysed a significantly weaker signal from the derivative chromosome 6 compared to the normal homologue, and a weak signal was also present on the marker chromosome (fig. 2C). However, the signals from the normal and deleted chromosome 6 homologues of patient 1 were of similar intensity (fig. 2D).

Fine mapping of the distal deletion breakpoint in patient 1 was a prerequisite for the intended cloning of the proximal breakpoint using inverse PCR. Array CGH suggested that the distal breakpoint mapped to intron 1 of the *MYO6* gene, within a 3.5-kb DNA stretch proximal to nucleotide 76,555,196. Sequence analysis of a series of PCR products of genomic DNA spanning known SNPs and/or possible STRs showed that patient 1 was heterozygous for SNP rs2748963 (G/T) at nucleotide 76,559,033 while all markers in the 10.5-kb interval proximal to this SNP were non-informative (homo- or hemizygous). Heterozygosity for SNP rs2748963 was retained in LR-PCR products extending to nucleotide 76,554,600. This nucleotide was located at the distal end of a 3-kb long contiguous cluster of various Alu and L1 repeats (fig. 3). This information together with the array data indicated that the distal deletion breakpoint in patient 1 was most likely located within this repetitive element cluster, precluding the use of inverse PCR for cloning of the proximal breakpoint located in the centromeric heterochromatin.

In patient 2 the proximal breakpoint mapped between the *IMPG1* and *HTR1B* genes, and the distal breakpoint was located in intron 1 of *FUT9*. The deletion junction was bridged with a LR-PCR product. Sequencing of this DNA fragment showed that the deletion joined nucleotides 77,231,427 and 96,635,141, with 7 nucleotides not belonging to any of the breakpoints added at the junction

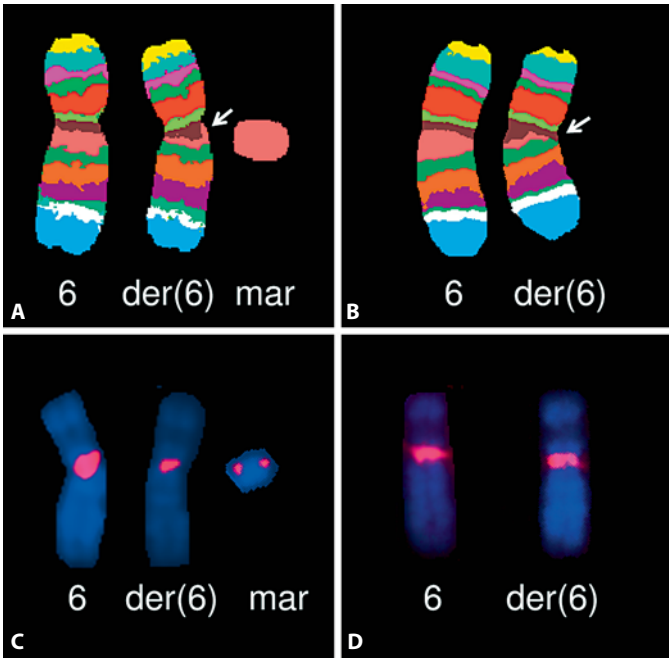

Fig. 2. mBAND analysis of chromosome 6 in the mother of patient 1 (**A**) and in patient 2 (**B**), and FISH analysis of chromosome 6 centromere in the mother of patient 1 (**C**) and in patient 1 (**D**). The mBAND analyses showed small deletions of proximal 6q (arrows) in both cases (**A**, **B**). The marker chromosome in the mother of patient 1 consisted of proximal 6q material deleted from the derived chromosome 6 (**A**). The signals of the chromosome 6 centromeric probe were present both on the deleted homologue and the marker (2 signals may suggest a double ring chromosome) in the mother of patient 1, and the signal on the deleted homologue was weaker than that on the normal chromosome 6 (**C**). In patient 1 no difference in signal intensity could be observed (**D**).

(fig. 3). No low copy repeats or dispersed repetitive elements were involved in the breakpoints, and their sequences had no homology (fig. 3).

Discussion

To our knowledge, 20 patients with deletions affecting the proximal 6q region and possibly extending to the adjacent part of middle 6q have been analyzed using array CGH and described in the literature [Le Caignec et al., 2005; Klein et al., 2007; Bonaglia et al., 2008; Derwinska et al., 2009; Lespinasse et al., 2009; Traylor et al., 2009; Wang et al., 2009; Spreiz et al., 2010; Woo et al., 2010] or the Decipher database [Firth et al., 2009] (fig. 4). Most of these patients were analysed using low-resolution arrays, and in none of them an attempt was made to clone the

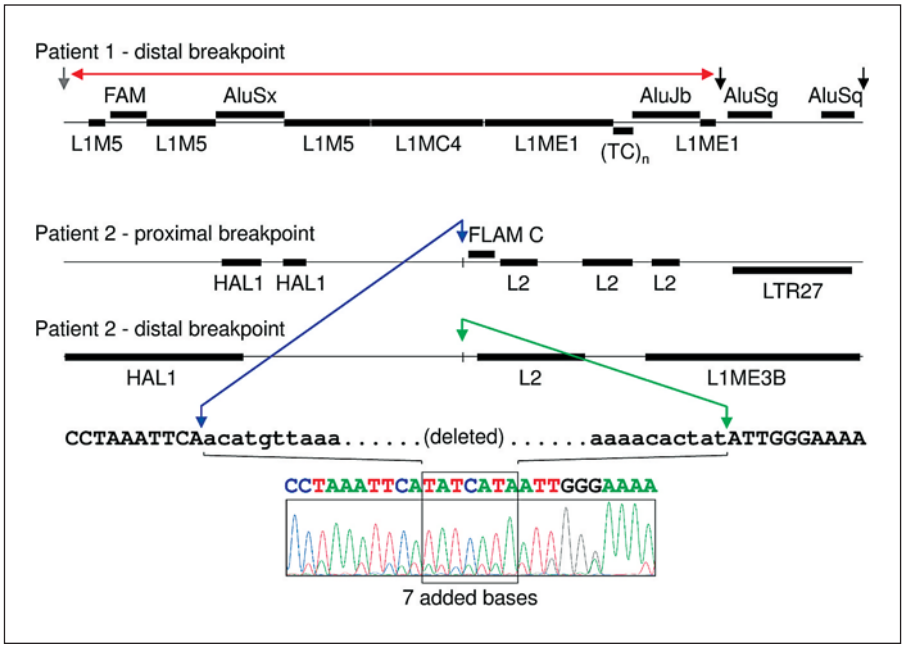

Fig. 3. Repeats at the distal deletion breakpoint in patient 1 and repeat content and sequence of both breakpoints in patient 2. LINE repeats in the 3.5-kb regions around the breakpoints are drawn on the line, SINE repeats above and other repeats below the line. In patient 1 (with the proximal breakpoint in the centromere gap), the distal breakpoint could be mapped only approximately to a cluster of repeats (red horizontal double arrow). The gray arrow marks the position very likely to be single-copy based on the array CGH data. The right black arrow points to heterozygous SNP rs2748963, and heterozygosity was retained on LR-PCR products extending to the position marked by the left black arrow. In patient 2 both the proximal (blue arrows) and distal breakpoints (green arrows) were located in repeat-poor regions. DNA sequencing showed that 7 bases were added at the junction. The deleted sequence is in lowercase.

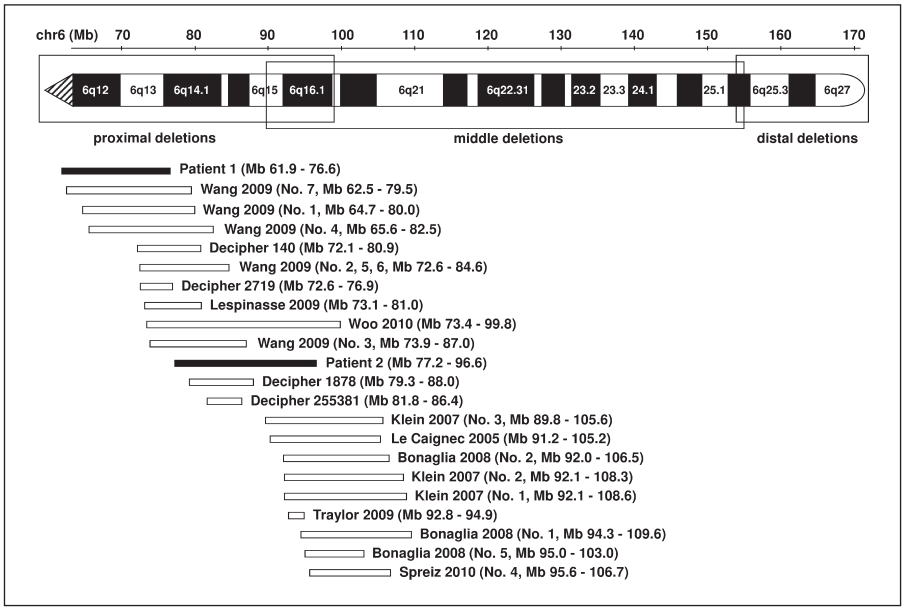

Fig. 4. Alignment of deletions in patients 1 and 2 with published deletions. Only patients with deletions not associated with other rearrangements, fine mapped using array methods and overlapping with but not extending significantly the region covered by deletions in our patients, were included. The ideogram on top shows the classification of 6q deletions.

deletion breakpoints and to elucidate the mechanisms of the aberrations.

The aberration in the mother of our patient 1 was likely caused by centromere fission. This mechanism of parallel formation of a deleted chromosome and a marker, most often a ring chromosome derived from the deleted material, was proposed by Barbara McClintock in 1938 and recently suggested to be referred to by her name [Baldwin et al., 2008]. The marker probably compensated for the deletion and caused the normal phenotype of the mother. However, due to its likely ring structure and the inherent instability of rings [Kosztolanyi, 1987], this marker was present only in a mosaic state, and was not transmitted or was lost in the early development of patient 1. About a dozen of patients who inherited an unbalanced karyotype from a parent with a balanced constitu-

tion involving centromere misdivision have been described [reviewed in Burnside et al., 2011]. Interestingly, while in the mother the centromeric signal from the deleted chromosome 6 was significantly weaker than that from the normal homologue, possibly reflecting the centromere fission, both chromosomes 6 in patient 1 showed signals of equal intensity, which could indicate some kind of healing or regaining of the centromeric alpha satellite arrays on the deleted chromosome. This and the absence of any new constriction on the deleted chromosome suggests that in this case the amount of the alpha satellite material retained on the deleted chromosome was sufficient to support the centromere function. This contrasted with a recently published similar event on chromosome 8 which, however, resulted in neocentromere formation [Burnside et al., 2011].

The distal deletion breakpoint in patient 1 likely involved a dense cluster of dispersed repeats rich in transposable sequences which precluded the cloning of the deletion junction. Interestingly, LINEs and SINEs are known to be present at increased frequency in the arrays of the centromeric alpha satellite repeats [Ugarkovic, 2009], and thus non-allelic homologous recombination may have played a role in the formation of this aberration [Lupski and Stankiewicz, 2005]. On the contrary, the absence of homology and different repeat content in the vicinity of the deletion breakpoints in patient 2 argued against non-allelic homologous recombination as the mechanism causing the aberration. The presence of 7 newly added bases at the deletion junction could be a signature of non-template directed repair associated with non-homologous end joining [Lupski and Stankiewicz, 2005].

The deletions in our 2 patients did not overlap and subdivided the proximal 6q region into 2 parts of almost equal length (fig. 4). The phenotypic abnormalities in our patients were of remarkably different severity. While the phenotype of patient 1 was relatively mild compared to the previously published cases and patient 2, the phenotype of patient 2 was more severe than that of other patients with proximal 6q deletions. Major anomalies were more often described in patients with middle or distal 6q deletions [Hopkin et al., 1997]. As the boundary between the proximal and middle 6q deletions was not exactly defined [Hopkin et al., 1997], the deletion in patient 2 might overlap with the region of the middle deletions.

The deletion of the distal part of proximal 6q in patient 2 may had more severe consequences due to the higher gene density in this region. Although the deletions in patients 1 and 2 were of similar size, the number of genes deleted in patient 2 was almost a double of that in patient 1. Both deletions were too large and with too many genes to allow assigning of individual symptoms to specific genes. Neither of our patients showed symptoms of recessive disorders caused by genes located in the region (*EYS*, *LMBRD1,* and *SLC17A5* in patient 1, and *LCA5*, *BCKDHB*, *SLC35A1,* and *RARS2* in patient 2) indicating lack of mutations on the remaining alleles of these genes. Interestingly, at the age when they were last examined, the patients also did not show any recognizable symptoms of dominant disorders mapping to the deletions: multiple epiphyseal dysplasia type 6 *(COL9A1)* [Czarny-Ratajczak et al., 2001], cone-rod dystrophy type 7 *(RIMS1)* [Johnson et al., 2003], and autosomal dominant nonsyndromic sensorineural hearing loss *(MYO6)* [Melchionda et al., 2001] in patient 1, and autosomal dominant atrophic macular degeneration *(ELOVL4)* [Bernstein et al., 2001; Zhang et al., 2001] in patient 2. The disorders can have a later onset, but other published deletion cases also showed no symptoms, indicating that these disorders may result from gain-of-deleterious-function mutations, although truncating mutations have also been described in at least some of them [Bernstein et al., 2001; Melchionda et al., 2001; Zhang et al., 2001]. Multiple genes in both deletions were good candidates for the developmental delay and mental retardation observed in both patients (e.g. *KHDRBS2*, *BAI3*, *B3GAT2*, *KCNQ5,* and *FILIP1* in patient 1, and *HTR1B*, *ORC3L*, *GABRR1*, *GABRR2,* and *EPHA7* in patient 2).

Some of the genotype-phenotype correlations were contradictory. A study of a small deletion involving only 2 genes suggested that the defect of *EPHA7* could negatively affect brain size and shape and lead to microcephaly. However, microcephaly was not observable in all patients with deletions overlapping the *EPHA7* locus [Traylor et al., 2009], and patient 2, who also has the *EPHA7* gene deleted, rather showed macrocephaly. This implies that some symptoms may be masked by the general population variability, and/or that the effect of some genes can be overridden by the effects of other loci deleted together with the specific gene.

Alignment of individual symptoms observed in our patients and other deletion carriers described in the literature indicated that hydronephrosis and other urinary tract defects might be enriched in patients with deletions overlapping middle 6q13, and similarly other symptoms could be assigned to deletions of other subregions (joint laxity and umbilical hernia to 6q14.1, cleft palate to 6q15, and various eye problems to 6q16.1). Similarly, while macrostomia was prevailing in patients with deletions of

the proximal part of the region studied, microstomia was characteristic for the distal part; and the same applied to upslanting and downslanting palpebral fissures. No obvious candidate genes for these phenotypes could be identified in these regions. Obesity could be characteristic for defects in the *SIM1* gene in the Prader-Willi-like candidate region of 6q16 [Bonaglia et al., 2008], which is distal to the region deleted in our patient 2. However, careful alignment of the published phenotypes also showed that the patients often clustered according to the author of the report rather than the chromosome region deleted, further stressing the importance of standardized phenotyping.

It can be expected that the widespread use of microarray and next-generation sequencing technologies will lead to the identification of small aberrations in patients with less complex phenotypes, which will be more informative for the correlation of individual symptoms with specific genes in the proximal 6q region.

Acknowledgements

Supported by grants MZOFNM2005, MZOVFN2005, and CHERISH (EC FP7 223692). The study makes use of data generated by the DECIPHER Consortium (http://decipher.sanger.ac.uk) funded by the Wellcome Trust.

References

Baldwin EL, May LF, Justice AN, Martin CL, Ledbetter DH: Mechanisms and consequences of small supernumerary marker chromosomes: from Barbara McClintock to modern genetic-counseling issues. Am J Hum Genet 82:398–410 (2008).

Bernstein PS, Tammur J, Singh N, Hutchinson A, Dixon M, et al: Diverse macular dystrophy phenotype caused by a novel complex mutation in the *ELOVL4* gene. Invest Ophthalmol Vis Sci 42:3331–3336 (2001).

Bonaglia MC, Ciccone R, Gimelli G, Gimelli S, Marelli S, et al: Detailed phenotype-genotype study in five patients with chromosome 6q16 deletion: narrowing the critical region for Prader-Willi-like phenotype. Eur J Hum Genet 16:1443–1449 (2008).

Burnside RD, Ibrahim J, Flora C, Schwartz S, Tepperberg JH, et al: Interstitial deletion of proximal 8q including part of the centromere from unbalanced segregation of a paternal deletion/marker karyotype with neocentromere formation at 8p22. Cytogenet Genome Res 132:227–232 (2011).

Czarny-Ratajczak M, Lohiniva J, Rogala P, Kozlowski K, Perala M, et al: A mutation in *COL9A1* causes multiple epiphyseal dysplasia: further evidence for locus heterogeneity. Am J Hum Genet 69:969–980 (2001).

Derwinska K, Bernaciak J, Wisniowiecka-Kowalnik B, Obersztyn E, Bocian E, et al: Autistic features with speech delay in a girl with an approximately 1.5-Mb deletion in 6q16.1, including *GPR63* and *FUT9*. Clin Genet 75: 199–202 (2009).

Firth HV, Richards SM, Bevan AP, Clayton S, Corpas M, et al: DECIPHER: Database of Chromosomal Imbalance and Phenotype in Humans Using Ensembl Resources. Am J Hum Genet 84:524–533 (2009).

Hopkin RJ, Schorry E, Bofinger M, Milatovich A, Stern HJ, et al: New insights into the phenotypes of 6q deletions. Am J Med Genet 70: 377–386 (1997).

Johnson S, Halford S, Morris AG, Patel RJ, Wilkie SE, et al: Genomic organisation and alternative splicing of human *RIM1*, a gene implicated in autosomal dominant cone-rod dystrophy (CORD7). Genomics 81:304–314 (2003).

Klein OD, Cotter PD, Moore MW, Zanko A, Gilats M, et al: Interstitial deletions of chromosome 6q: genotype-phenotype correlation utilizing array CGH. Clin Genet 71:260–266 (2007).

Kosztolanyi G: Does 'ring syndrome' exist? An analysis of 207 case reports on patients with a ring autosome. Hum Genet 75:174–179 (1987).

Le Caignec C, Swillen A, Van Asche E, Fryns JP, Vermeesch JR: Interstitial 6q deletion: clinical and array CGH characterisation of a new patient. Eur J Med Genet 48:339–345 (2005).

Lespinasse J, Gimelli S, Bena F, Antonarakis SE, Ansermet F, et al: Characterization of an interstitial deletion 6q13-q14.1 in a female with mild mental retardation, language delay and minor dysmorphisms. Eur J Med Genet 52: 49–52 (2009).

Lupski JR, Stankiewicz P: Genomic disorders: molecular mechanisms for rearrangements and conveyed phenotypes. PLoS Genet 1:e49 (2005).

Melchionda S, Ahituv N, Bisceglia L, Sobe T, Glaser F, et al: *MYO6*, the human homologue of the gene responsible for deafness in Snell's waltzer mice, is mutated in autosomal dominant nonsyndromic hearing loss. Am J Hum Genet 69:635–640 (2001).

Spreiz A, Muller D, Zotter S, Albrecht U, Baumann M, et al: Phenotypic variability of a deletion and duplication 6q16.1–q21 due to a paternal balanced ins(7;6)(p15;q16.1q21). Am J Med Genet A 152A:2762–2767 (2010).

Traylor RN, Fan Z, Hudson B, Rosenfeld JA, Shaffer LG, et al: Microdeletion of 6q16.1 encompassing *EPHA7* in a child with mild neurological abnormalities and dysmorphic features: case report. Mol Cytogenet 2:17 (2009).

Ugarkovic DI: Centromere-competent DNA: structure and evolution. Prog Mol Subcell Biol 48:53–76 (2009).

Wang JC, Dang L, Lomax B, Turner L, Shago M, et al: Molecular breakpoint mapping of 6q11-q14 interstitial deletions in seven patients. Am J Med Genet A 149A:372–379 (2009).

Woo KS, Kim JE, Kim KE, Kim MJ, Yoo JH, et al: A de novo proximal 6q deletion confirmed by array comparative genomic hybridization. Korean J Lab Med 30:84–88 (2010).

Zhang K, Kniazeva M, Han M, Li W, Yu Z, et al: A 5-bp deletion in *ELOVL4* is associated with two related forms of autosomal dominant macular dystrophy. Nat Genet 27:89–93 (2001).

Twin Research and Human Genetics
Volume 17 ▌ Number 5 ▌ pp. 405–410 ▌ © The Authors 2014 ▌ doi:10.1017/thg.2014.29

Monozygotic Twins with 17q21.31 Microdeletion Syndrome

Marketa Vlckova,[1,#] Miroslava Hancarova,[1,#] Jana Drabova,[1] Zuzana Slamova,[1] Monika Koudova,[1,*] Renata Alanova,[1,] Katrin Mannik,[2] Ants Kurg,[2] and Zdenek Sedlacek[1]**

[1]Department of Biology and Medical Genetics, Charles University 2nd Faculty of Medicine and University Hospital Motol, Prague, Czech Republic

[2]Institute of Molecular and Cell Biology, University of Tartu, Tartu, Estonia

Chromosome 17q21.31 microdeletion syndrome is a genomic disorder caused by a recurrent 600 kb long deletion. The deletion affects the region of a common inversion present in about 20% of Europeans. The inversion is associated with the H2 haplotype carrying additional low-copy repeats susceptible to non-allelic homologous recombination, and this haplotype is prone to deletion. No instances of 17q21.31 deletions inherited from an affected parent have been reported, and the deletions always affected a parental chromosome with the H2 haplotype. The syndrome is characterized clinically by intellectual disability, hypotonia, friendly behavior and specific facial dysmorphism with long face, large tubular or pear-shaped nose and bulbous nasal tip. We present monozygotic twin sisters showing the typical clinical picture of the syndrome. The phenotype of the sisters was very similar, with a slightly more severe presentation in Twin B. The 17q21.31 microdeletion was confirmed in both patients but in neither of their parents. Potential copy number differences between the genomes of the twins were subsequently searched using high-resolution single nucleotide polymorphism (SNP) and comparative genome hybridisation (CGH) arrays. However, these analyses identified no additional aberrations or genomic differences that could potentially be responsible for the subtle phenotypic differences. These could possibly be related to the more severe perinatal history of Twin B, or to the variable expressivity of the disorder. In accord with the expectations, one of the parents (the mother) was shown to carry the H2 haplotype, and the maternal allele of chromosome 17q21.31 was missing in the twins.

■ **Keywords:** 17q21.31 microdeletion syndrome, monozygotic twins, CNV, epigenetics

The chromosome 17q21.31 microdeletion syndrome (Koolen-de Vries syndrome, MIM 610443) is a genomic disorder characterized by intellectual disability (ID), friendly behavior, hypotonia and distinct facial features with thin long face, large pear-shaped nose and prominent chin (Koolen et al., 2006; Sharp et al., 2006; Shaw-Smith et al., 2006). The typical facial phenotype is usually less apparent in the infancy and becomes remarkable during adolescence (Koolen et al., 2008; Slavotinek, 2008). Major anomalies, seizures, joint hyperlaxity and eye anomalies can be also present, but are less common. The prevalence of the syndrome is estimated to 1 in 16,000 (Koolen et al., 2008).

The syndrome is caused by a recurrent 600 kb deletion of 17q21.31. The region is predisposed to rearrangement by its specific genome architecture. The deletion breakpoints map to large clusters of low copy repeats (LCRs) predisposing to non-allelic homologous recombination (NAHR). The 17q21.31 region is known for its inversion polymorphism of about 900 kb and the presence of two highly divergent SNP haplotypes designated H1 and H2. H2 is associated with the inversion and is found at a frequency of 20% in the European population (Stefansson et al., 2005). H2 differs from the non-inverted H1 allele by the arrangement of LCRs, which makes H2 prone to NAHR events (Koolen et al., 2008; Steinberg et al., 2012). At least one of the parents of deletion patients always carried at least one H2

RECEIVED 26 June 2013; ACCEPTED 5 September 2013. First published online 9 June 2014.

ADDRESS FOR CORRESPONDENCE: Miroslava Hancarova, Department of Biology and Medical Genetics, Charles University 2nd Faculty of Medicine and University Hospital Motol, Plzenska 130/221, 15000 Prague 5, Czech Republic. E-mail: miroslava.hancarova@lfmotol.cuni.cz

# These authors contributed equally to the work.

* Present address: GHC Genetics, Prague, Czech Republic

** Present address: Institute for the Care of Mother and Child, Prague, Czech Republic

allele, which seems to be necessary for the deletion formation. The deletion encompasses several genes, among which haploinsufficiency of *KANSL1* has recently been shown to be responsible for the syndrome (Koolen et al., 2012b; Zollino et al., 2012).

Herein we present the first report of monozygotic twins carrying the 17q21.31 microdeletion and showing only slightly different phenotypes. Analysis on high-resolution arrays did not reveal any genetic differences between the twins. The subtle clinical differences can probably be explained by different perinatal history of the twins or by the variable expressivity of the disorder.

Materials and Methods

Patients

The girls were born from a twin pregnancy to healthy, non-consanguineous parents of Czech origin. The age of the mother and father were 22 and 25 years, respectively. The delivery was in the 38th week of gestation by cesarean section due to hypoxia in Twin B.

Twin A was born with a weight of 1980 g and length of 43 cm (both below the 3rd centile). The Apgar score was 3-7-7 (Apgar, 1953). Partial exchange transfusion had to be administered due to polyglobulia and hyperviscosity syndrome. The newborn suffered from left-side hypotonic hydronephrosis with reflux. Twin B was born with a weight of 1910 g and length of 43 cm (both below the 3rd centile). The Apgar score was 3-7-7. Perinatal hypoxia followed by intracranial hemorrhage occurred during the delivery. Right-side hydronephrosis, strabismus and horizontal nystagmus were noted in the newborn.

Postaxial polydactyly of toes and fingers, congenital hip dysplasia, delay in motor milestones and speech delay were observed in both twins. Psychological examination at the age of 10 years showed moderate ID in both twins, but Twin A performed slightly better than Twin B (Twin A was assessed as functioning in the upper range of moderate ID and being slightly more diligent and adaptable, and less anxious). At the examination at 19 years of age both twins had disproportionately short stature (Twin A 153.3 cm, the 1st centile; Twin B 157.7 cm, the 6th centile) with shortening of upper and lower limbs, thoracic hyperkyphosis, low-pitched voice and similar facial expression (Figure 1), and with very long, thin and coarse face, coarse hair, thick eyebrows, large nose, bulbous nasal tip, smooth broad philtrum, thick lips, mandibular prognathism, and hirsutism. Twin A had a high palate. Twin B had wide-spaced teeth and diastema, and slightly more coarse facial features compared to Twin A. However, especially with respect to their age, the overall clinical picture of both twins was remarkably similar. None of them showed other symptoms often described in the 17q21.31 microdeletion syndrome, such as seizures, joint hypermobility, cleft lip/palate, heart defects, or pectus excavatum (Koolen et al., 2012b).

Laboratory Analyses

Informed consent for genetic analyses was obtained from the parents of the patients. Genomic DNA of both twins and the parents was extracted from blood lymphocytes using the Gentra Puregen Blood Kit (Qiagen, Hilden, Germany) according to the manufacturer's protocol. Conventional cytogenetic analysis was performed using standard G-banding. The *FMR1* gene testing used the Fragile X PCR Kit (Abbot, Abbot Park, IL, USA). The BAC array comparative genome hybridisation (CGH; BlueGnome, Cambridge, UK) analysis of Twin A was performed according to the manufacturer's instructions. The FISH analysis with the BAC clone RP11-111L23 (BlueGnome) was used to independently confirm the deletion in the twins and to test for its presence in the parents. Diagnostic alleles of single nucleotide polymorphisms (SNPs) rs1800547 (G) and rs9468 (C) and the presence of the 238 bp deletion in intron 9 of the *MAPT* gene characteristic for the H2 allele (Koolen et al., 2008) were analysed in the family using DNA sequencing and gel electrophoresis, respectively (PCR primer sequences are available upon request). The high-resolution SNP array analysis of both twins using the HumanCytoSNP-12 BeadChip (~300 K; Illumina, San Diego, CA, USA) and direct array CGH comparison of their genomes using the Nimblegen 2.1M Whole-Genome CGH Array (Roche NimbleGen, Madison, WI, USA) were used for confirmation of monozygosity and for a more detailed analysis of potential differences in copy number variants (CNVs) in the genomes of both twins. Data were analysed using GenomeStudio (Illumina), QuantiSNP (Colella et al., 2007) and SignalMap (Roche NimbleGen). Multiplex ligation-dependent probe amplification (MLPA) analysis was performed using custom synthetic probes and the P200 Human DNA Reference Probemix (MRC Holland, Amsterdam, The Netherlands; probe sequences are available upon request). All analyses used genome build hg18/NCBI36.

Results

The cytogenetic analysis revealed normal female karyotypes, and the *FMR1* gene testing excluded the fragile X syndrome in both twins. The BAC array CGH analysis of Twin A identified a deletion characteristic for the 17q21.31 microdeletion syndrome with breakpoints between bases 40,740,861-41,074,265 and 41,679,148-42,178,065. The FISH analysis confirmed the deletion in both twins but in neither of their parents. The haplotype analysis revealed homozygosity for the inverted H2 allele in the mother, homozygosity for the non-inverted H1 allele in the father, and hemizygosity for H1 in both twins. Thus the deletion was *de novo* in the twins and it affected one of the maternal chromosomes 17.

The SNP array analysis confirmed the monozygosity of the twins. This high-resolution analysis found no differences in the extent of the 17q21.31 microdeletion between

FIGURE 1

(Colour online) Facial photographs of the patients at the age of 19 (top) and 23 years (bottom). Twin A is on the left, Twin B on the right. Features typical for the 17q21.31 microdeletion syndrome (long, narrow and coarse face, coarse hair, large nose with bulbous nasal tip, broad philtrum, thick lips, mandibular prognathism) and subtle differences between the twins (slightly more coarse facial features in Twin B) can be observed.

the patients (chr17:41,041,709-41,560,151; Figure 2). Both twins shared two additional CNVs, a 0.1 Mb long duplication in 10q26.3 (chr10:135,102,337-135,215,135) encompassing *CYP2E1*, and a 1.7 Mb long deletion in 16p11.2 (chr16:31,977,497-33,704,396) involving *TP53TG3*. Both these CNVs were located in highly polymorphic copy-number variable regions. The analysis with the highest resolution used (2.1M array CGH) did not detect any obvious CNV differences between the genomes of the twins. In several small regions copy number differences between the patients could not be excluded (chr18:14,184,640-15,370,613 and chr21:13,302,864-14,139,384 being most suspicious), but most of these segments coincided with complex segmental duplications, where the validity of the findings was questionable, impossible to confirm using standard methods and of uncertain clinical impact even if they were confirmed. The analysis of three of these regions where unique sequences could be targeted with custom MLPA probes (chr14:18,127,587-19,272,166; chr16:32,082,491-34,128,024 and chr22:49,414,658-49,584,579) failed to confirm any copy number differences between the twins in these regions.

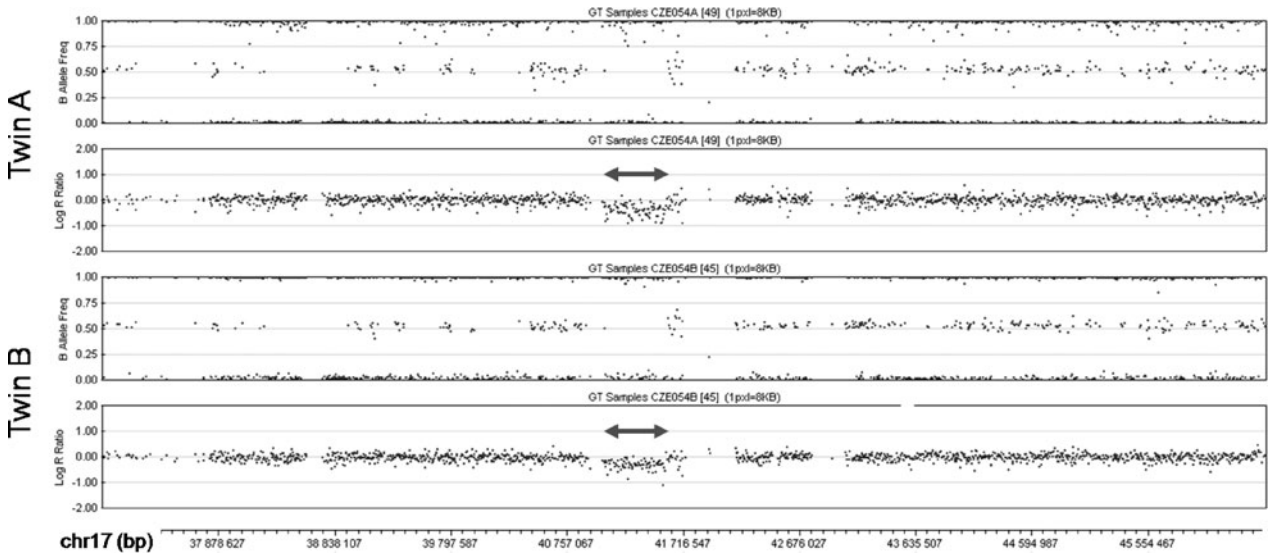

FIGURE 2

SNP array analysis of the middle part of 17q in the patients. The deletions are marked by double arrows. In the diagrams of the B Allele Frequency (top panel in each twin) deletions are indicated by the absence of dots around the value of 0.5 (absence of heterozygous genotype AB). Concurrently, in the diagrams of Log R Ratio (bottom panel in each twin) the deletions are indicated by dots clustering below the value of 0.0 (decreased intensity of the signal).

Discussion

To our knowledge this is the first description of monozygotic twins with the 17q21.31 microdeletion syndrome. The deletion was *de novo* on a maternal chromosome 17, although a low-level somatic and gonadal mosaicism could not be excluded (Koolen et al., 2012a). The twin sisters showed only a subtle phenotypic discordance. Generally, discordant monozygotic twins are a valuable resource for the analysis of genetic, epigenetic or environmental variation contributing to the disease. The 17q21.31 microdeletion syndrome is one of a few clinically recognizable new syndromes with well-defined clinical outcome, and rare instances of affected twins could contribute to understanding the variability of this disorder.

The phenotypes of our patients were very similar and fully corresponded to the typical picture of the syndrome (Koolen et al., 2008). The subtle phenotypic differences between the twins included a slightly more severe cognitive impairment and more coarse facial features with strabismus and horizontal nystagmus in Twin B. These differences prompted us to search for possible genomic differences. The 17q21.31 microdeletion was of the same size in both twins, and also the two other CNVs detectable at the 300K level were present in common and were unlikely to contribute to the phenotype. The 10q26.3 duplication encompassing *CYP2E1* is a common polymorphism possibly associated with alcohol addiction (Deng & Deitrich, 2008). The 16p11.2 deletion around *TP53TG3* affected a very variable gene-poor pericentric region. Also, the direct comparison of both genomes using an even higher resolution (2.1M) did not yield any findings. Several suspicious CNV differences were located in highly polymorphic regions of segmental duplications, the structure of which made the confirmation of these aberrations difficult or impossible, and analysis of three of these regions failed to confirm any differences between the two genomes. However, it should be noted that these regions are susceptible to *de novo* events, and that any genomic differences between the twins could be expected to be in a mosaic state, further complicating their detection. In any case, due to the paucity of genes, these potentially differential CNVs were unlikely to affect the phenotype.

Several other studies focused on monozygotic twins with microdeletion syndromes and a different degree of phenotypic discordance. Ghebranious et al. (2007) presented monozygotic twins with a 16p11.2 microdeletion and no other CNV differences, who showed similar phenotypes but severe aortic stenosis developed only in one twin. Most monozygotic twin pairs reported with 22q11 deletions were also phenotypically discordant. Singh et al. (2002) reviewed five such pairs in whom no high-resolution whole genome analyses were performed to uncover potential genomic differences. The discordance in a recently identified monozygotic twin pair with a 22q11 microdeletion was explained by size differences of the deletions (Halder et al., 2012), which however have not been confirmed using an independent method and are thus questionable. Rio et al. (2013) reported a phenotypically and genetically discordant monozygotic twin pair carrying a 2p25.3 deletion in one twin and mosaicism with one third of cells with the 2p25.3 deletion, one third with a 2p25.3 duplication, and one third of normal cells in the other one. Other recent studies of monozygotic twin pairs discordant for breast cancer (Lasa et al., 2010),

schizophrenia (Ono et al., 2010) or congenital heart defect (Breckpot et al., 2012) also identified no CNV differences explaining the discordance.

In the absence of genetic differences, the twin discordance can be explained by epigenetics or environment (Czyz et al., 2012). The study of *DRD2* methylation in two pairs of monozygotic twins, one discordant and one concordant for schizophrenia, showed that the affected twin from the discordant pair was epigenetically 'closer' to the affected concordant twins than to his unaffected co-twin (Petronis et al., 2003). Similarly, the affected twin from a monozygotic pair discordant for caudal duplication anomaly showed higher methylation of the *AXIN1* promoter than the unaffected twin, whose *AXIN1* methylation was higher than that of normal controls (Oates et al., 2006). An epigenome-wide approach found that approximately one third of monozygotic twins had epigenetic differences in DNA methylation and histone modification (Fraga et al., 2005). Epigenetic marks were more distinct in twins who were older, had different lifestyles, and had spent less of their lives together, underlining the significant role of environmental factors in the process (Fraga et al., 2005; Kaminsky et al., 2009). Environmental factors could include the differences in the intrauterine environment and in perinatal and postnatal history, and the twinning process itself could play a role as well as stochastic factors can do (Czyz et al., 2012). Mosaicism resulting from later postzygotic genomic rearrangements or epigenetic changes can be difficult to detect, and it can differentially affect specific tissues (e.g., the brain) that are not accessible to testing. Another limitation of twin studies, including ours, which are using blood as the source of DNA, is blood chimerism, which can mask genetic or epigenetic discordance (Erlich, 2011).

In the case of our patients who show no CNV differences, all other factors mentioned above could contribute to their subtle phenotypic discordance. The currently emerging whole exome and whole genome sequencing approaches could identify possible genetic variation on the nucleotide level not addressed in our study, and epigenetic differences could also play a role. However, the simplest and likely sufficient explanation of the slightly discordant phenotype of the twins is in their perinatal history, which was clearly more severe in Twin B (perinatal hypoxia followed by intracranial hemorrhage). The differences in the clinical picture of our patients can also be the consequence of stochastic factors acting in the common inter-individual variability, and the variable expressivity of the 17q21.31 microdeletion syndrome.

Acknowledgments

We thank the family of the patients for cooperation. Supported by grants CHERISH 223692 and CZ.2.16/3.1.00/24022 from the European Commission, DRO UH Motol 00064203 and NT/14200 from the Czech Ministry of Health, and SF0180027s10 from the Estonian Ministry of Education and Research.

References

Apgar, V. (1953). A proposal for a new method of evaluation of the newborn infant. *Current Researches in Anesthesia & Analgesia*, *32*, 260–267.

Breckpot, J., Thienpont, B., Gewillig, M., Allegaert, K., Vermeesch, J. R., & Devriendt, K. (2012). Differences in copy number variation between discordant monozygotic twins as a model for exploring chromosomal mosaicism in congenital heart defects. *Molecular Syndromology*, *2*, 81–87.

Colella, S., Yau, C., Taylor, J. M., Mirza, G., Butler, H., Clouston, P., ... Ragoussis, J. (2007). QuantiSNP: An objective Bayes Hidden-Markov model to detect and accurately map copy number variation using SNP genotyping data. *Nucleic Acids Research*, *35*, 2013–2025.

Czyz, W., Morahan, J. M., Ebers, G. C., & Ramagopalan, S. V. (2012). Genetic, environmental and stochastic factors in monozygotic twin discordance with a focus on epigenetic differences. *BMC Medicine*, *10*, 93.

Deng, X. S., & Deitrich, R. A. (2008). Putative role of brain acetaldehyde in ethanol addiction. *Current Drug Abuse Reviews*, *1*, 3–8.

Erlich, Y. (2011). Blood ties: Chimerism can mask twin discordance in high-throughput sequencing. *Twin Research and Human Genetics*, *14*, 137–143.

Fraga, M. F., Ballestar, E., Paz, M. F., Ropero, S., Setien, F., Ballestar, M. L., ... Esteller, M. (2005). Epigenetic differences arise during the lifetime of monozygotic twins. *Proceedings of the National Academy of Science of the U S A*, *102*, 10604–10609.

Ghebranious, N., Giampietro, P. F., Wesbrook, F. P., & Rezkalla, S. H. (2007). A novel microdeletion at 16p11.2 harbors candidate genes for aortic valve development, seizure disorder, and mild mental retardation. *American Journal of Medical Genetics Part A*, *143A*, 1462–1471.

Halder, A., Jain, M., Chaudhary, I., & Varma, B. (2012). Chromosome 22q11.2 microdeletion in monozygotic twins with discordant phenotype and deletion size. *Molecular Cytogenetics*, *5*, 13.

Kaminsky, Z. A., Tang, T., Wang, S. C., Ptak, C., Oh, G. H., Wong, A. H., ... Petronis, A. (2009). DNA methylation profiles in monozygotic and dizygotic twins. *Nature Genetics*, *41*, 240–245.

Koolen, D. A., Dupont, J., de Leeuw, N., Vissers, L. E., van den Heuvel, S. P., Bradbury, A., ... Parker, M. J. (2012a). Two families with sibling recurrence of the 17q21.31 microdeletion syndrome due to low-grade mosaicism. *European Journal of Human Genetics*, *20*, 729–733.

Koolen, D. A., Kramer, J. M., Neveling, K., Nillesen, W. M., Moore-Barton, H. L., Elmslie, F. V., ... de Vries, B. B. (2012b). Mutations in the chromatin modifier gene KANSL1 cause the 17q21.31 microdeletion syndrome. *Nature Genetics*, *44*, 639–641.

Koolen, D. A., Sharp, A. J., Hurst, J. A., Firth, H. V., Knight, S. J., Goldenberg, A., ... de Vries, B. B. (2008). Clinical

and molecular delineation of the 17q21.31 microdeletion syndrome. *Journal of Medical Genetics*, *45*, 710–720.

Koolen, D. A., Vissers, L. E., Pfundt, R., de Leeuw, N., Knight, S. J., Regan, R., ... de Vries, B. B. (2006). A new chromosome 17q21.31 microdeletion syndrome associated with a common inversion polymorphism. *Nature Genetics*, *38*, 999–1001.

Lasa, A., Ramon y Cajal, T., Llort, G., Suela, J., Cigudosa, J. C., Cornet, M., ... Baiget, M. (2010). Copy number variations are not modifiers of phenotypic expression in a pair of identical twins carrying a BRCA1 mutation. *Breast Cancer Research and Treatment*, *123*, 901–905.

Oates, N. A., van Vliet, J., Duffy, D. L., Kroes, H. Y., Martin, N. G., Boomsma, D. I., ... Chong, S. (2006). Increased DNA methylation at the AXIN1 gene in a monozygotic twin from a pair discordant for a caudal duplication anomaly. *American Journal of Human Genetics*, *79*, 155–162.

Ono, S., Imamura, A., Tasaki, S., Kurotaki, N., Ozawa, H., Yoshiura, K., & Okazaki, Y. (2010). Failure to confirm CNVs as of aetiological significance in twin pairs discordant for schizophrenia. *Twin Research and Human Genetics*, *13*, 455–460.

Petronis, A., Gottesman, II, Kan, P., Kennedy, J. L., Basile, V. S., Paterson, A. D., & Popendikyte, V. (2003). Monozygotic twins exhibit numerous epigenetic differences: Clues to twin discordance? *Schizophrenia Bulletin*, *29*, 169–178.

Rio, M., Royer, G., Gobin, S., de Blois, M., Ozilou, C., Bernheim, A., ... Malan, V. (2013). Monozygotic twins discordant for submicroscopic chromosomal anomalies in 2p25.3 region detected by array CGH. *Clinical Genetics*, *84*, 31–36.

Sharp, A. J., Hansen, S., Selzer, R. R., Cheng, Z., Regan, R., Hurst, J. A., ... Eichler, E. E. (2006). Discovery of previously unidentified genomic disorders from the duplication architecture of the human genome. *Nature Genetics*, *38*, 1038–1042.

Shaw-Smith, C., Pittman, A. M., Willatt, L., Martin, H., Rickman, L., Gribble, S., ... Carter, N. P. (2006). Microdeletion encompassing MAPT at chromosome 17q21.3 is associated with developmental delay and learning disability. *Nature Genetics*, *38*, 1032–1037.

Singh, S. M., Murphy, B., & O'Reilly, R. (2002). Monozygotic twins with chromosome 22q11 deletion and discordant phenotypes: Updates with an epigenetic hypothesis. *Journal of Medical Genetics*, *39*, e71.

Slavotinek, A. M. (2008). Novel microdeletion syndromes detected by chromosome microarrays. *Human Genetics*, *124*, 1–17.

Stefansson, H., Helgason, A., Thorleifsson, G., Steinthorsdottir, V., Masson, G., Barnard, J., ... Stefansson, K. (2005). A common inversion under selection in Europeans. *Nature Genetics*, *37*, 129–137.

Steinberg, K. M., Antonacci, F., Sudmant, P. H., Kidd, J. M., Campbell, C. D., Vives, L., ... Eichler, E. E. (2012). Structural diversity and African origin of the 17q21.31 inversion polymorphism. *Nature Genetics*, *44*, 872–880.

Zollino, M., Orteschi, D., Murdolo, M., Lattante, S., Battaglia, D., Stefanini, C., ... Marangi, G. (2012). Mutations in KANSL1 cause the 17q21.31 microdeletion syndrome phenotype. *Nature Genetics*, *44*, 636–638.

ELSEVIER

Array comparative genome hybridization in patients with developmental delay: two example cases

Research Paper

Miroslava Hancarova, Jana Drabova, Zuzana Zmitkova, Marketa Vlckova, Petra Hedvicakova, Drahuse Novotna, Zdenka Vlckova, Sarka Vejvalkova, Tatana Marikova and Zdenek Sedlacek

Department of Biology and Medical Genetics, Charles University, 2nd Faculty of Medicine and University Hospital Motol, V Uvalu 84, Prague, Czech Republic

Developmental delay is often a predictor of mental retardation (MR) or autism, two relatively frequent developmental disorders severely affecting intellectual and social functioning. The causes of these conditions remain unknown in most patients. They have a strong genetic component, but the specific genetic defects can only be identified in a fraction of patients. Recent developments in genomics supported the establishment of the causal link between copy number variants in the genomes of some patients and their affection. One of the techniques suitable for this analysis is array comparative genome hybridization, which can be used both for detailed mapping of chromosome rearrangements identified by classical cytogenetics and for the identification of novel submicroscopic gains or losses of genetic material. We illustrate the power of this approach in two patients. Patient 1 had a cytogenetically visible deletion of chromosome X and the molecular analysis was used to specify the gene content of the deletion and the prognosis of the child. Patient 2 had a seemingly normal karyotype and the analysis revealed a small recurrent deletion of chromosome 1 likely to be responsible for his phenotype. However, the genetic dissection of MR and autism is complicated by high heterogeneity of the genetic aberrations among patients and by broad variability of phenotypic effects of individual genetic defects.

Introduction

Child development is a process of acquiring skills in several domains (cognitive, social, emotional, speech/language, and motor) during specific time periods. Developmental delay is defined as significant delay in two or more domains, and is thought to predict a future diagnosis of mental retardation (MR) and/or autism [1]. MR is a disability with limitations in intellectual functioning and adaptive behavior diagnosed before the age of 18 years [2]. It can be classified into four categories: mild (IQ 50–70), moderate (IQ 35–50), severe (IQ 20–35), and profound (IQ < 20). Autism is a disorder characterized by impairments of social interaction and communication, and unusual, often stereotyped behavior and interests [2]. Around 0.5–1% and 2–3% of population suffer from autism and MR, respectively [3–5]. Both conditions can be syndromic (if associated with other symptoms like facial dysmorphy) or non-syndromic (if no other consistent clinical or metabolic features are present).

Autism and MR affect the brain, the most complex human organ, and their causes are therefore also complex. Environmental factors include maternal infections or drug use in pregnancy and perinatal complications [4,5]. However, the genetic component is much more important in both conditions, as shown in twin and family studies [6,7]. Defined genetic syndromes, mutations in several specific genes, and cytogenetically visible or submicroscopic chromosome aberrations currently account for about 20% of the cases, but these causes are very heterogeneous with no one specific genetic defect being responsible for more than 1–2% of the cases [3,8,9].

Corresponding author: Sedlacek, Z. (zdenek.sedlacek@lfmotol.cuni.cz)

1871-6784/$ - see front matter doi:10.1016/j.nbt.2010.10.006

If autism and MR were polygenic or multifactorial, the causal alleles could be detectable by whole-genome association studies. However, the results of these studies were rather disappointing because of low odds ratio and low level of replication [3]. Nevertheless, these analyses pointed to a more frequent occurrence of copy number variants (CNVs) in patients with autism and MR. CNVs are variably deleted or amplified regions of the genome, often involving genes. This variability is likely to contribute to phenotypic variability including the predisposition to diseases or the occurrence of cognitive and behavioral disorders or congenital defects [10,11].

The association of autism and MR with rare CNVs led to a shift in the understanding these two conditions from the multifactorial model (based on an interplay of common genetic variants with low effect) to the multiple rare variant model. Most affected individuals may carry unique genetic defects with strong effect, often arising *de novo* [8,9]. This model also explains the difficulties of whole-genome association studies to identify the predisposing loci, possibly just with regions containing clustering of different rare variants giving positive scores [12].

CNVs are detected using genomic approaches including array comparative genome hybridization (aCGH), which has underwent a remarkable shift in genome coverage and resolution since its first description [13,14]. In patients with defects identified using karyotyping (which has a resolution limit of several Mb), aCGH can specify the extent of the rearrangement and more precisely map the breakpoints. In cytogenetically normal patients, aCGH can reveal submicroscopic gains or losses of chromosome material. In both cases aCGH can point to genes potentially causing the phenotypes, and help to identify the mechanisms of the rearrangements.

In this report we illustrate the power of aCGH in two patients with developmental delay. In the first patient a large deletion was identified using karyotyping and aCGH allowed the determination of its exact size and gene content which had immediate consequences for the prognosis in this patient. In the second patient with a seemingly normal karyotype, the aCGH analysis revealed a small cytogenetically invisible deletion likely to be responsible for his phenotype.

Materials and methods

Patients

Patient 1 was admitted to the hospital at the age of six weeks with an electrolyte imbalance, renal failure and elevated levels of creatine kinase, adrenocorticotropic hormone and liver markers. He also suffered from hyponatremia, dehydration, proteinuria, high level of glycerol in the urine and weak spontaneous mobility. At a follow-up check at the age of two years he showed mild psychomotor retardation. His parents were healthy and the family history was not remarkable.

Patient 2 had a remarkable family history of MR and congenital defects (Fig. 1). At the age of 12 years, the boy (III.1) suffered from mild MR, attention deficit hyperactivity disorder (ADHD) with autistic features and microcephaly. After birth he presented with hypotonia, and his psychomotor development was disharmonic. His mother (II.2) also suffered from delayed development in childhood and showed behavioral problems and mental deficit. Both she and her maternal half-sister (II.4) suffered from congenital defects

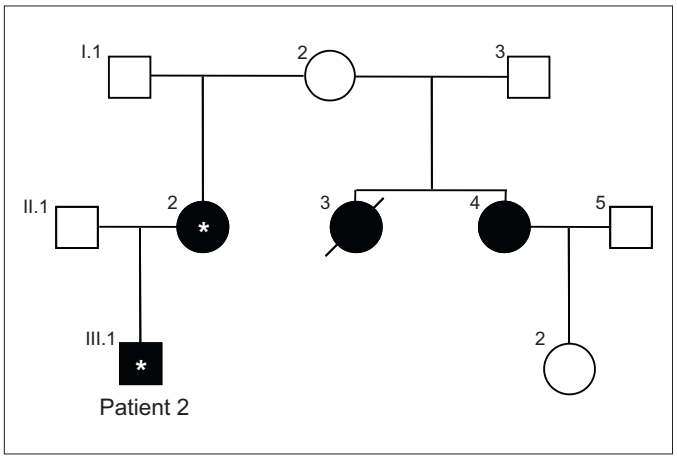

FIGURE 1

Pedigree of the family of Patient 2. Individuals with MR and/or congenital defects (see text for details) are represented by black symbols, and those in whom the deletion was identified are marked with asterisks. DNA from other family members was not available for study.

(syndactyly and cleft palate, respectively). Another maternal half-sister (II.3) with multiple malformations (caudal regression, gastroschisis, anal atresia and colon agenesis, persistent cloaca, and meningocele) died soon after birth. Their mother, the grandmother of the patient (I.2), had no remarkable phenotype. Only the DNA of Patient 2 and his mother were available for testing.

Laboratory methods

Chromosomal aberrations in peripheral blood lymphocytes of the patients and their parents were analyzed using standard cytogenetic techniques. Further delineation of the aberrations was performed using fluorescence in situ hybridization (FISH) with a chromosome X painting probe (WCP X, Cytocell) in Patient 1, and a locus-specific probe (RP11-533N14, BlueGnome) in Patient 2, according to the recommendations of the manufacturer.

Genomic DNA was isolated from blood lymphocytes of the patients and their parents using the Gentra Puregene Blood Kit (Qiagen). Multiplex ligation-dependent probe amplification (MLPA) was performed using the SALSA MLPA KIT P034/P035 DMD/Becker (MRC-Holland) according to the instructions of the manufacturer. Whole-genome aCGH analysis of Patient 2 was performed using a bacterial artificial chromosome (BAC) array with median backbone probe spacing of 565 kb (CytoChip V3, BlueGnome) according to the instructions of the manufacturer. Custom high resolution aCGH analysis of Patient 1 and Patient 2 was performed by Nimblegen on catalogue oligonucleotide CGH arrays specific for chromosome X (HG18_CHRX_FT, median probe spacing of 340 bp) and chromosome 1 (HG18_CHR1_FT, median probe spacing of 541 bp), respectively. The results were analyzed using the SignalMap software (Nimblegen). Long-range PCR used the Expand Long Template PCR System (Roche). The gene content of the deletions was analyzed using the UCSC and Ensembl genome browsers (http://genome.ucsc.edu/cgi-bin/hgGateway, http://www.ensembl.org/index.html) and the hg18 assembly.

Results

The phenotype of Patient 1 and his biochemical findings were suggestive of glycerol kinase deficiency (GKD) and Duchenne

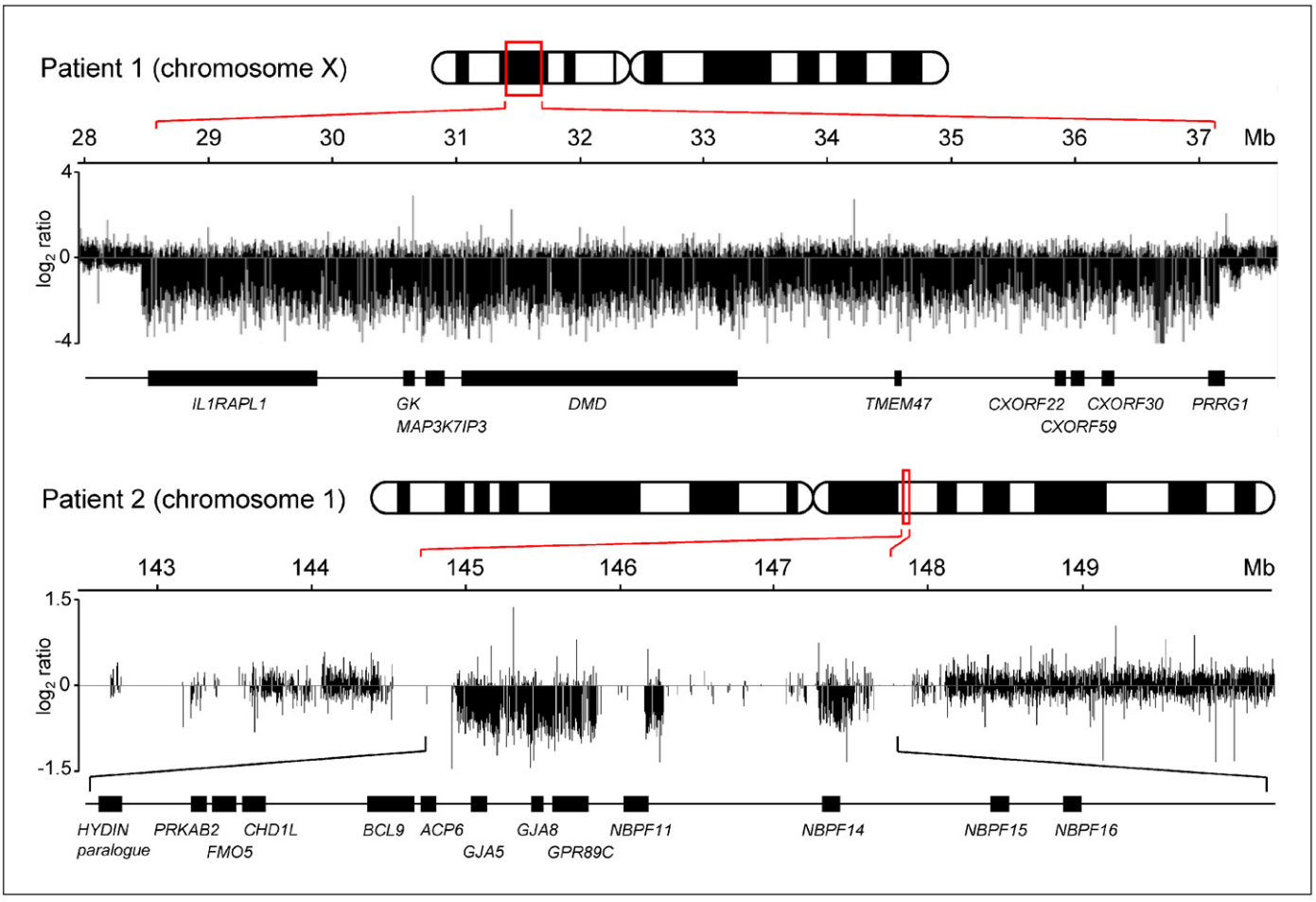

FIGURE 2

The results of aCGH analysis of the deletions in Patient 1 and Patient 2 using chromosome-specific high resolution arrays. The regions of decreased signal ratios correspond to the deletions. This analysis allowed precise mapping of the breakpoints (which was not possible using karyotyping and low resolution arrays used initially to identify the deletions in Patient 1 and Patient 2, respectively), and the assessment of gene content of the deletions. Regions devoid of signals correspond to segmental duplications and low-copy repeats not represented on the chromosome 1 specific array.

muscular dystrophy (DMD). This prompted us to perform cytogenetic analysis aimed primarily at deletions of the X chromosome. Indeed, his karyotype was 46,XY,del(X)(p21.2p21.3), and the deletion was likely to encompass the above-mentioned two loci. The same deletion was also identified in his asymptomatic mother. FISH analysis showed that the deleted segment was not translocated to any other chromosome. MLPA analysis of the *DMD* gene of Patient 1 revealed a deletion of all exons, and classical PCR analysis indicated the deletion of several additional genes (*GK*, *NR0B1* and *IL1RAPL1*). aCGH analysis confirmed an 8.7 Mb long deletion between Mb 28.5 and 37.2 of the X chromosome containing a total of nine protein coding genes (Fig. 2). The distal breakpoint of the deletion was located between the *DCAF8L1* and *IL1RAPL1* genes, and the proximal breakpoint was located in the *PRRG1* gene. Both breakpoints mapped to regions of unique DNA or dispersed repeats and there was no obvious homology between the breakpoint regions. Repeated attempts to clone the deletion junction using long-range PCR were not successful.

The karyotype of Patient 2 was normal, but the low resolution aCGH analysis showed a deletion of chromosome region 1q21.1. While the signals from BACs RP11-373C9 and RP11-763B22 were normal, BAC RP11-94I2 yielded a borderline signal, and low signals from BACs RP11-47D6, RP11-563P13, RP11-441L11, RP11-533N14, RP11-314N2 and RP11-301M17 clearly indicated a deletion. The remaining chromosomes did not show any copy number aberrations. The deletion was fine mapped using high resolution aCGH to Mb 144.8–147.8 of chromosome 1 (Fig. 2). The size of the deletion was about 3 Mb and it contained 13 protein coding genes. Both breakpoints were located in extended complex regions of segmental duplication and low-copy repeats. The deletion was confirmed in Patient 2 using FISH with BAC probe RP11-533N14, and the same technique was used to identify the same deletion in his mother.

Discussion

The results obtained in our patients clearly illustrate the power of aCGH for the detailed analysis of cytogenetically visible defects and for the detection of rare submicroscopic CNVs associated with developmental delay, autism and MR.

The molecular analyses in Patient 1 confirmed the suspected diagnosis of a rare X-linked recessive disorder, complex GKD. In contrast to isolated GKD, which is caused by point mutations in the glycerol kinase gene (*GK*), complex GKD is a contiguous gene

syndrome caused by a deletion of the *GK* locus together with other Xp21 sequences including the adrenal hypoplasia congenita locus (*NR0B1* gene) and/or *DMD* [15]. About 100 patients with complex GKD have been reported, and their phenotypes usually reflected the variable size of their deletions. The analysis of gene content of the deletions is therefore an important prognostic factor. Patient 1 carried a rather large deletion including the *IL1RAPL1* gene, which has been associated with MR and autism [16,17], and his prognosis with respect to these two conditions was therefore rather unfavorable. In accord with this prognosis, Patient 1 showed at the age of 2 years mild psychomotor retardation. The breakpoints of the deletion were unique and contained no segmental duplications or low-copy repeats.

A genetic basis of the phenotype and the remarkable family history of Patient 2 was suspected but completely unknown. The molecular analysis using whole-genome aCGH identified a submicroscopic deletion of chromosome 1 in the distal 1q21.1 region, which was subsequently fine mapped using high resolution aCGH. This recently described microdeletion is recurrent, and its formation is mediated by recombination between segmental duplications flanking the deleted region [18,19]. In large collections of affected individuals this deletion has been associated with a complex and variable phenotype which often included MR and autism or ADHD, microcephaly and a wide range of other congenital anomalies. This deletion removes several protein coding genes including a paralog of the *HYDIN* gene which is suspected to cause microcephaly and other neuropsychiatric features in the deletion carriers [18]. The deletion of 1q21.1 is often inherited from a less affected or even seemingly normal parent [18,19]. The mildly affected mother of Patient 2 was shown to carry the deletion, and the family history suggested that also her two half-sisters could be carriers. Their unaffected mother, the grandmother of Patient 2, could also carry the deletion, or at least a germline mosaic of this defect.

Patient 2 illustrates very clearly several key problems of the recent concept of genetics of autism and MR. First, there is a very substantial heterogeneity at the phenotype level, and the clinical picture of carriers of a particular genetic defect can be very variable, even within one family. The phenotypic spectrum in 1q21.1 deletion carriers ranges from completely normal individuals through various mild to fully expressed psychiatric phenotypes to very severe congenital defects [18,19], and this is similar for other CNVs. The reason for this variability is generally unknown but it is speculated that the genetic background (the genotype of the individual at other genome loci), epigenetic status and interaction with environmental triggers are playing the key role [20]. It has been proposed recently that full phenotypic expression of one CNV can be dependent on the co-occurrence of other CNVs in the same individual [21]. Second, the spectrum of genetic defects underlying autism and MR in individual patients can be extremely broad, and individual genetic defects can be extremely rare. Although the microdeletion of 1q21.1 has clearly been associated with autism and MR, its frequency among affected individuals reaches only 0.2–0.5% [18,19], and thus the diagnostic yield of this rearrangement is very low. The same applies to most other genetic defects currently known to be responsible for these conditions [3,8,9]. This precludes the possibility to design a simple targeted diagnostic genetic test. It is probable that the continuing improvements and increasing affordability of high resolution genome analysis methods including whole-genome sequencing will soon lead to the identification of the 'missing heritability' in an increasing fraction of sufferers from complex diseases, and will at the same time offer efficient tools for their routine diagnostics.

Acknowledgements

Supported by grants MZOFNM2005 from the Ministry of Health of the Czech Republic, and INCORE (FP6 043318) and CHERISH (FP7 223692) from the European Commission.

References

1 Accardo, P. and Capute, A. (1995) Intellectual disability. In *Principles and Practice of Pediatrics* (Oski, F. and Diangelis, C.D., eds), pp. 673–679, Lippincott, Philadelphia

2 American Psychiatric Association, (1994) *Diagnostic and Statistical Manual of Mental Disorders (DSM-IV)* (4th ed.), American Psychiatric Association, Washington DC

3 Abrahams, B.S. and Geschwind, D.H. (2008) Advances in autism genetics: on the threshold of a new neurobiology. *Nat. Rev. Genet.* 9, 341–355

4 Levy, S.E. *et al.* (2009) Autism. *Lancet* 374, 1627–1638

5 Roeleveld, N. *et al.* (1997) The prevalence of mental retardation: a critical review of recent literature. *Dev. Med. Child Neurol.* 39, 125–132

6 Jorde, L.B. *et al.* (1991) Complex segregation analysis of autism. *Am. J. Hum. Genet.* 49, 932–938

7 Bailey, A. *et al.* (1995) Autism as a strongly genetic disorder: evidence from a British twin study. *Psychol. Med.* 25, 63–77

8 Buxbaum, J.D. (2009) Multiple rare variants in the etiology of autism spectrum disorders. *Dialog. Clin. Neurosci.* 11, 35–43

9 Vissers, L.E. *et al.* (2010) Genomic microarrays in mental retardation: from CNV to gene, from research to diagnosis. *J. Med. Genet.* 47, 285–297

10 Iafrate, A.J. *et al.* (2004) Detection of large-scale variation in the human genome. *Nat. Genet.* 36, 949–951

11 Conrad, D.F. *et al.* (2010) Origins and functional impact of copy number variation in the human genome. *Nature* 464, 704–712

12 Dickson, S.P. *et al.* (2010) Rare variants create synthetic genome-wide associations. *PLoS Biol.* 8, e1000294

13 Chen, X. *et al.* (2009) New tools for functional genomic analysis. *Drug Discov. Today* 14, 754–760

14 Solinas-Toldo, S. *et al.* (1997) Matrix-based comparative genomic hybridization: biochips to screen for genomic imbalances. *Genes Chromos. Cancer* 20, 399–407

15 Sjarif, D.R. *et al.* (2000) Isolated and contiguous glycerol kinase gene disorders: a review. *J. Inherit. Metab. Dis.* 23, 529–547

16 Piton, A. *et al.* (2008) Mutations in the calcium-related gene IL1RAPL1 are associated with autism. *Hum. Mol. Genet.* 17, 3965–3974

17 Carrie, A. *et al.* (1999) A new member of the IL-1 receptor family highly expressed in hippocampus and involved in X-linked mental retardation. *Nat. Genet.* 23, 25–31

18 Brunetti-Pierri, N. *et al.* (2008) Recurrent reciprocal 1q21.1 deletions and duplications associated with microcephaly or macrocephaly and developmental and behavioral abnormalities. *Nat. Genet.* 40, 1466–1471

19 Mefford, H.C. *et al.* (2008) Recurrent rearrangements of chromosome 1q21.1 and variable pediatric phenotypes. *N. Engl. J. Med.* 359, 1685–1699

20 Manolio, T.A. *et al.* (2009) Finding the missing heritability of complex diseases. *Nature* 461, 747–753

21 Girirajan, S. *et al.* (2010) A recurrent 16p12.1 microdeletion supports a two-hit model for severe developmental delay. *Nat. Genet.* 42, 203–209